Difference in tolerance to anti-hyperalgesic effect and its molecular mechanisms between chronic treatment with morphine and fentanyl under the chronic pain-like state

2007

Satoshi Imai

A dissertation submitted in partial fulfillment of the requirements leading to the degree of Doctor (Pharmacy) presented to the Department of Toxicology, Hoshi University School of Pharmacy and Pharmaceutical Sciences, Tokyo, Japan

This dissertation is dedicated to my parents, my sister and my wife Masumi.

Table of Contents

Abbreviations

Amino acid residues

Ser: Serine

Thr: Threonine

Chemical substances and drugs

AS-ODN: Antisense oligodeoxynucleotide

β-FNA : β-Funaltrexamine

CFA: Complete Freund's adjuvant

DAMGO: [D-Ala^2,*N*-Me-Phe^4,Gly^5-ol]enkephalin

DPDPE: Cyclic-[D-Pen^2, D-Pen^5] enkephalin

EGTA: Ethylene glycol-bis (2-aminoethylether)-*N*,*N*,*N'*,*N'*-tetraacetic acid

GDP: Guanosine-5'-diphosphate

[^{35}S]GTPγS: Guanosine-5'-o-(3-[^{35}S]thio)triphosphate

MM-ODN: Mismatch oligodeoxynucleotide

nor-BNI: Nor-binaltorphimine hydrochloride

NTI: Naltrindole methanesulfonate

PTX: Pertussis toxin

SDS: Sodium dodecyl sulfate

U-50,488H: Trans-3,4-dichloro-N-(2-(1-pyrrolidinyl)-cyclohexyl)benzene-acetamide

Buffers

PBS: Phosphate-buffered saline

TBS: Tris-buffered saline

TTBS: Tween 20-TBS

Endogenous substances

β_2-MG: β_2-Microglobulin

GABA: γ-Aminobutyric acid

Enzymes and intracellular messengers

CaMKII: Ca^{2+}/calmodulin-dependent protein kinase II

GRK: G-protein coupled receptor kinase

GRK2: G protein-coupled receptor kinase 2

IP_3: Inositol (1,4,5)-triphosphate

MAPK: Mitogen-activated protein kinase

p-PKA: Phosphorylated-protein kinase A

PKC: Protein kinase C

PKCγ: Protein kinase C γ

PLC: Phospholipase C

p-PKC: Phosphorylated-PKC

PP2A: Protein phosphatase 2A

p-PP2A: Phosphorylated-protein phosphatase 2A

SDS: Sodium dodecyl sulfate

Receptors

DOR: δ-Opioid receptor

GPCR: G-protein coupled receptor

KOR: κ-Opioid receptor

MOR: μ-Opioid receptor

p-MOR: Phosphorylated μ-opioid receptor

Injection route

i.c.v.: Intracerebroventricular

i.t.: Intrathecal

s.c.: Subcutaneous

Others

ANOVA: Analysis of variance

CNS: Central nervous system

EC_{50}: 50% effective concentration

ED_{50}: 50% effective dose

IC50: 50% inhibitory concentration

IR: Immunoreactivity

PAG: Periaqueductal gray matter

RT-PCR: Reverse transcription-polymerase chain reaction

S.E.M.: Standard error mean

UTR: Untranslated region

WHO: World Health Organization

Structures of drugs used in the present study

Morphine hydrochloride

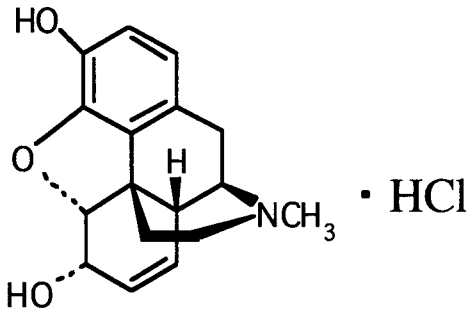

· HCl

Fentanyl citrate

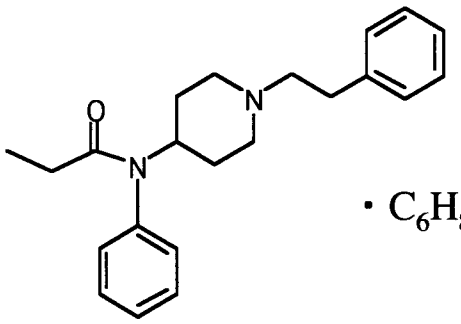

· $C_6H_8O_7$

DAMGO: [D-Ala^2,*N*-Me-Phe^4,Gly^5-ol]enkephalin

Tyr-D-Ala-Gly-NMe-Phe-Gly-ol

Endomorphin-1

Tyr-Pro-Trp-Phe-NH_2

β-FNA: β-Funaltrexamine

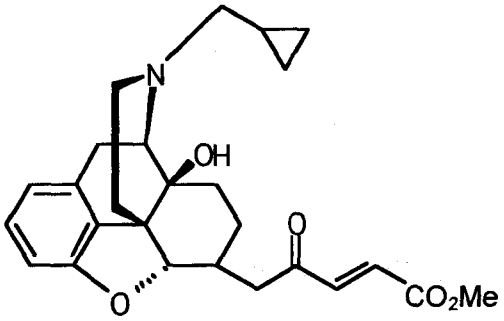

NTI: Naltrindole methanesulfonate

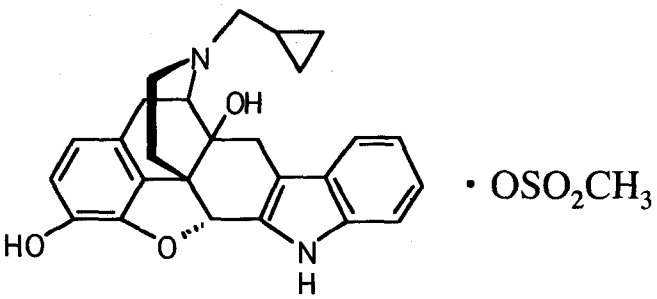

U-50,488H: Trans-3,4-dichloro-N-(2-(1-pyrrolidinyl)-cyclohexyl) benzene-acetamide

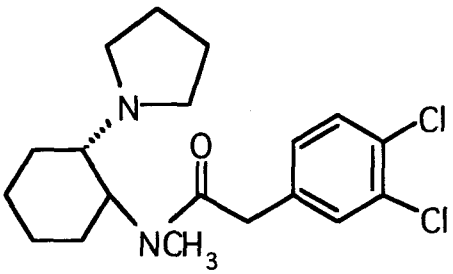

DPDPE: Cyclic-[D-Pen^2, D-Pen^5] enkephalin

H-Tyr-D-Pen-Gly-Phe-D-Pen-OH

nor-BNI: Nor-binaltorphimine hydrochloride

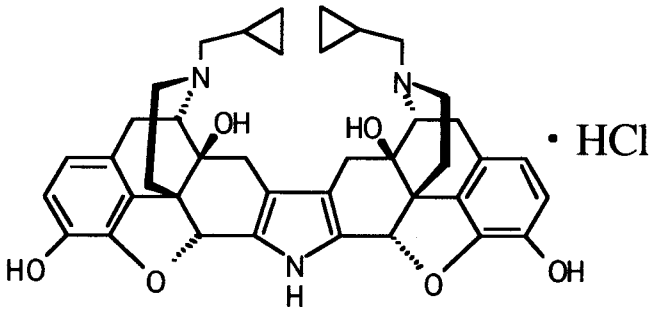

General introduction

μ-Opioid receptors

Pharmacological studies using the peptide and alkaloid opioid receptor ligands have identified several types of opioid receptors, including μ, δ and κ [1-3]. In the year 1992, a δ-opioid receptor (DOR) was first cloned by two independent groups, Evans et al. [4] and Kieffer et al. [5]. Following the cloning of the DOR, the μ-opioid receptor (MOR) and κ-opioid receptor (KOR) have been cloned in the past several years [6-9]. The studies on cDNA clone encoding structurally related receptor with amino acid have suggested the similarity of these three receptor genes as high as 65% [10,11]. The cloning of these opioid receptor types revealed that they are members of the G-protein-coupled receptor (GPCR) superfamily. Opioid receptors are coupled to pertussis toxin-sensitive Gi/o protein, which are linked functionally to inhibition of adenylyl cyclase activity, activation of receptor-operated K^+ currents, and suppression of voltage-gated Ca^{2+} currents [12-14]. Recently, it has been demonstrated that opioid receptors may be coupled to other second messenger systems, including activation of the mitogen-activated protein kinase (MAPK) and the phospholipase C (PLC)/ inositol (1,4,5)-triphosphate (IP_3)/protein kinase C (PKC)-mediated cascade, through the βγ subunits of their G proteins [15-17]. Actions of MOR agonists have been subdivided into μ_1- and μ_2-opioid receptor mechanisms, based upon the effect of the selective μ_1-opioid receptor antagonist naloxonazine [18]. It has long been considered that μ_1-opioid receptors mediate antinociception supraspinally, whereas μ_2-opioid receptors are

responsible for spinal antinociception. However, no report on the identification of μ_1 and μ_2 subtypes at the molecular level has been provided so far.

Splice variant-dependent MOR subtypes

Many GPCR genes contain introns, which introduce the possibility of variants due to alternative splicing. Variations in gene-product splicing occur at the level of processing of heteronuclear-RNAs in the cell nucleus. A growing body of evidence suggests that alternative splicing with 14 exons results in several spliced variants for the cloned MOR [19,20]. Several splice variant-dependent MOR subtypes that are different in length and amino acid composition only at the intracellular carboxyl terminus have been identified. Among the isolated variants, MOR-1 that has exon 1, 2, 3 and 4, and MOR-1B that contains an alternatively spliced exon 5 instead of the original exon 4 [21,22]. It was reported that the expression of MOR-1B mRNA can be observed in many brain areas. The highest concentrations of MOR-1B mRNA are detected in the frontal cortex and striatum, and the lowest concentrations are found in the olfactory bulb and the cerebellum [21]. Following agonist stimulation, MOR-1B shows an accelerated cycle of receptor endocytosis and reactivation, which in turn promotes a greater resistance to agonist-induced desensitization than MOR-1 [21-23].

In term of MOR-1C, the 12 amino acids encoded by exon 4 in MOR-1 are replaced by 52 amino acids derived from the combination of the new exons 7, 8 and 9, which are conserved exons among other two variants MOR-1E and -1F [24]. Previous immunohistochemical study demonstrated that intense MOR-1C-immunoreactivity

(IR) is observed in the hypothalamic nuclei and lateral septum, whereas moderate MOR-1-IR is presented in these regions. Conversely, MOR-1-IR is found abundantly in the striatum, whereas no expression of MOR-1C is observed in the same region [25]. It has been proposed that MOR-1C shows the rapid receptor desensitization, whereas little or no internalization is caused following prolonged exposure to MOR agonists [26]. Considering these findings, it can be speculated that individual splice variants derived from the same MOR gene partially differ in their functional roles in the expression of MOR agonist-induced pharmacological actions.

The use of opioids to treat chronic pain

The primary afferent nociceptor is generally the initial structure involved in nociceptive processes. The primary afferent fibers associated with transmission nociceptive signals to the substantia gelatinosa in the dorsal horn can be grouped into two main categories: small myelinated (A-δ) and unmyelinated (C) sensory afferent fibers [27,28]. Second-order neurons ascend the spinal cord to terminate in many supraspinal structures throughout the brain stem, thalamus and cortex. In the thalamus, it is well-known that these systems are divided into two main groups such as ventrobasal complex and intralaminar nuclei.[29] Former including the ventral posterolateral nuclei and ventral posteromedial nuclei, is involved in the sensory discriminative component of pain and further projects to the somatosensory cortex.[29-31] Latter including the central medial nuclei and parafascicular nucleus, amygdala and hippocampus, is associated with the affective motivational aspects of pain and projects

to the cingulate cortex. Chronic peripheral tissue inflammation often produces a state of neuropathic pain characterized by hyperalgesia (an exaggerated pain in response to painful stimuli) and allodynia (a pain evoked by normally innocuous stimuli). The development of neuropathic pain following peripheral tissue inflammation depends both on an increase in the sensitivity of these first synapses at the insite of inflammation and on an increase in the excitability of neurons in the central nervous system (CNS) [32-34]. Several animal models of neuropathic pain following peripheral tissue inflammation have been created for the investigation of mechanisms underlying the induction of neuropathic pain [35,36]. Complete Freund's adjuvant (CFA), carrageenan and formalin have been well documented to produce the state of inflammatory pain hypersensitivity in rodents following intraplantar injection.

Opioids have been used to treat patients with chronic pain. Recent clinical trials suggest that oxycodone, morphine and levorphanol can improve chronic pain such as diabetic peripheral neuropathy and postherpetic neuralgia [37]. In addition, early pharmacological studies have demonstrated that the microinjection of a typical MOR agonist morphine or endogenous MOR agonist endomorphin-1 into ventrolateral orbital cortex dramatically suppressed the state of inflammatory pain hypersensitivity in rodents [12]. On the contrary, several lines of clinical evidence have demonstrated that neuropathic pain is particularly difficult to treat, as it is only partially relieved by high doses of MOR agonists. These clinical experience are supported by findings that the antinociceptive effects by either subcutaneous (s.c.) or intrathecal (i.t.) treatment with morphine was attenuated in rodents with sciatic nerve ligation [12,13,38].

Furthermore, Narita et al. [39] showed previously that the phosphorylation of MOR, which leads to uncoupling with G-proteins, was clearly increased in the superficial laminae of the L5 lumbar spinal dorsal horn of the mice with chronic pain. Under these conditions, the morphine-induced antinociceptive effect was significantly suppressed in mice with chronic pain. Thus, the utility of opioids for neuropathic pain remains controversial. It is likely that the reason for the limited application of MOR agonists in the clinical environment is related to a poor understanding the analgesic properties of these MOR agonists under the pain-like state.

MOR agonists, morphine and fentanyl

According to the World Health Organization (WHO) guidelines for patients with moderate or severe cancer pain, morphine has been a "gold standard" for treatment of moderate to severe cancer pain. The i.t. administration of morphine has been the standard therapy to control long-term intractable pain. However, the use of morphine for the treatment of cancer pain is sometimes accompanied by side effects such as emesis, vomiting, sedation, papillary constriction, euphoria, constipation and drowsiness [40,41]. Quality of life has been shown to be significantly reduced in patients who experience morphine-induced side effects. In 1959, fentanyl, the anilidopiperidine class of MOR agonist, was reported as a potent synthetic analgesic with a lower propensity to produce these undesirable effects in the clinical setting [42]. Fentanyl is used for opioid rotation in the clinic and exhibits 50-100 times more potent analgesic activity and short duration of its action as compared to that of morphine.

The low molecular weight and lipid solubility of fentanyl make it possible for delivery via the transdermal therapeutic system. The transdermal therapeutic fentanyl-system allows for a continued and sustained titratable amount of fentanyl to be delivered without the inconvenience of the typical administration of other analgesics for 24 hr. However, it has been considered that the analgesic tolerance is the adverse effect in the pain management of pain with fentanyl [43]. The understanding of mechanism underlying the opioid side effects and the establishment of the strategy to prevent and manage them are essential skills for pain management.

Opioid tolerance and receptor turnover

The development of chronic tolerance is characteristic of all opioids with agonist activity, regardless of the receptor type with which they interact. Tolerance to opioids first becomes evident as a shortening of the duration of drug action and a diminution of the peak effects. The rate at which tolerance develops depends on the pattern of use and the characteristics of the opioids used. Significant tolerance only develops when there is a continuous drug action.

Tolerance can be described as an adaptation of a biological system to the repeated effects of a drug and defined as a loss of potency of a drug after its repeated administration. The processes underlying opioid tolerance involve complex compensatory changes in many opioid and non-opioid neuronal circuits. One major mechanism controlling GPCR responsiveness is the activation-dependent regulation of receptors, called homologous desensitization [44,45]. Other mechanisms also contribute

to intrinsic regulation of GPCR signaling. These mechanisms include receptor activation-independent regulation, called heterologous desensitization, which results from regulating and altering the signaling efficiency of downstream effectors [46,47]. Among homologous adaptive processes, the receptor desensitization, internalization and trafficking appears to play key role in the development of opioid tolerance. A number of studies demonstrated that long-term or repeated treatment with MOR agonists leads to the rapid receptor desensitization followed by internalization of MORs. A growing body of evidence suggests that the phosphorylation of MOR at diverse sites of its intracellular domain by G protein-coupled receptor kinase (GRK) or second messenger-regulated protein kinases such as PKC and Ca^{2+}/calmodulin-dependent protein kinase II (CaMKII) has been shown to trigger the internalization of phosphorylated MOR from the cell surface to the cytosol [48]. These processes are thought to be an important step toward receptor desensitization. Among diverse serine/threonine residues of intracellular domain of MOR, phosphorylation of serine (Ser) 375 in the mouse MOR is essential for its internalization. After phosphorylation of Ser/threonine (Thr) residues of the C-terminus, MORs are internalized via clathrin-coated pits into early endosomes and subsequently dephosphorylated by intracellular protein phosphatases. The dephosphorylated MORs might be either recycled through sorting endosomes back to the plasma membrane or transported to the lysosomes for degradation. It has been considered that opioid tolerance is, in part, the end results of a coordinated balance between processes governing desensitization and resensitization of MORs. However, the mechanisms underlying the development of tolerance to

MOR agonists have not been fully understood. Most previous studies concerning molecular events in opioid tolerance have been performed using the excessive dose of MOR agonists or several cell lines including the non-neural cell model. It seems likely that these previous experimental models are not necessarily correspond to actual situation of opioid tolerance observed in the clinic. Therefore, in order to further clarify properties and molecular mechanisms of analgesic tolerance, I should investigate the utility of repeated treatment with MOR agonists at optimal doses for the relief of pain associated with physiological change in endogenous MOR system and its related downstream signaling machinery.

CXBK recombinant inbred mice

To date, a number of studies concerning differences of the pharmacological property between morphine and fentanyl have been undertaken. Previous electrophysiological and biochemical studies have indicated that fentanyl and its analog sufentanil, but not morphine, reversibly suppressed sodium inward currents through the neuronal voltage-gated sodium channels [49]. Furthermore, it is well established that fentanyl induces internalization of MORs, whereas morphine does not promote detectable internalization of MORs in cultured cells. Thus, the individual pharmacological character of morphine or fentanyl is clearly different.

CXBK mice are recombinant inbred mice derived from a cross between the C57BL/6J and BALB/cJ strains. [50,51] Previous studies suggested that CXBK mice had a partial deficiency of MOR proteins and the level of MOR mRNA in the brain of CXBK

mice as compared to their progenitor mice and other outbred strains [52]. On the other hand, the densities of DOR and KOR appear to be relevantly unaffected by the deficiency of MORs in CXBK mice. The sequence of the coding region (1197 bases) of MOR mRNA of CXBK mice is identical to that of C57BL/6J mice. Within the 726 bases of 3'-untranslated region (UTR) and 241 bases of 5'-UTR of the MOR gene, a C/A polymorphism at 5'-UTR is the only difference between CXBK (C nucleotide) and C57BL/6J (A nucleotide) mice [53]. It has been well known that these genetic variation in UTR regions are known to affect the expression level of either the corresponding mRNA or protein without the influence upon its function [54]. The inheritance of MOR gene of CXBK mice was well correlated with its behavioral pharmacologic properties, which is less sensitivity to MOR agonists. Mizoguchi et al. [55] demonstrated that endogenous MOR agonists endomorphin-1 and endomorphin-2 increase guanosine-5'-o-(3-[^{35}S]thio)triphosphate ([^{35}S]GTPγS) binding to the pons/medulla membranes from C57BL/6J mice in a concentration-dependent manner. However, the increases of [^{35}S]GTPγS binding induced by either endomorphin-1 or endomorphin-2 in CXBK mice were significantly much lower than those in C57BL/6J mice. It is therefore worthwhile to use CXBK mice to further investigate the pharmacological profiles of MOR agonists such as morphine and fentanyl.

Aim and Scope

The aim of the present study was to investigate the molecular mechanism of the development of tolerance to anti-hyperalgesic effects between chronic treatment with morphine and fentanyl under the pain-like state. Therefore, behavioral, neurochemical and biochemical experiments were conducted in the present study.

The specific aims of the proposed research are:

In Chapter 1:

The aim of the present study was to investigate whether repeated *in vivo* administration of morphine or fentanyl could cause the development of tolerance to the morphine- or fentanyl-induced anti-hyperalgesic effect under the long-lasting pain-like state induced by intraplantar administration of CFA in mice. Additionally, I evaluated the effect of repeated administration of morphine and fentanyl on the regulatory process of MOR trafficking, which is responsible for receptor phosphorylation, internalization and recycling pathways, following CFA injection in mice.

In Chapter 2:

I investigated whether CXBK recombinant inbred mice, which are known to have a partial deficiency of MOR, could be deficient in a putative splice variant-dependent MOR subtype MOR-1B. Furthermore, I evaluated the functional role of supraspinal

MOR-1B in the endogenous MOR agonist endomorphin-1-induced antinociceptive effects.

In Chapter 3:

To clarify the antinociceptive properties of morphine and fentanyl in the mouse supraspinal and spinal cord, I investigated the effects of pretreatment with MOR, DOR and KOR antagonist, β-funaltrexamine (β-FNA), naltrindole methanesulfonate (NTI) and nor-binaltorphimine hydrochloride (nor-BNI), respectively, on the antinociceptive effects induced by morphine or fentanyl using the mouse tail-flick test. In addition, I compared 50% effective dose (ED_{50}) values for antinociceptive effects between morphine and fentanyl at peripheral, spinal and supraspinal site, respectively, in ICR mice. Finally, I investigated the specific involvement of MOR subtypes at either the spinal or supraspinal site with analgesic properties of morphine and fentanyl using CXBK mice.

Ethics

The present study was conducted in accordance with the Guiding Principles for the Care and Use of Laboratory Animals, as adopted by the Committee on Animal Research of Hoshi University, which is accredited by the Ministry of Education, Culture, Sports, Science and Technology of Japan. Every effort was made to minimize the numbers and any suffering of animals used in the following experiments. Animals were used only once in the present study.

Chapter 1

Differences in tolerance to anti-hyperalgesic effects between chronic treatment with morphine and fentanyl under the pain-like state

Introduction

Tolerance can be described as an adaptation of a biological system to the repeated effects of a drug and defined as a loss of potency of a drug after its repeated administration. The processes underlying antinociceptive tolerance involve complex compensatory changes in many opioid and non-opioid neuronal circuits. Among homologous adaptive processes, the receptor desensitization, internalization and trafficking appear to play the key role in the development of opioid tolerance [15,17]. A number of studies demonstrated that long-term or repeated treatment with MOR agonists leads to the rapid receptor desensitization followed by internalization of MORs. The initial process of these events is that the phosphorylation of intracellular domains of MOR by GRK or second messenger-regulated protein kinases such as PKC and CaMKII [15-17]. After phosphorylation of Ser/Thr residues of the C-terminus, MORs are internalized via clathrin-coated pits into early endosomes and subsequently dephosphorylated by intracellular protein phosphatases. The dephosphorylated MORs might be either recycled through sorting endosomes back to the plasma membrane or transported to the lysosomes for degradation. It has been considered that antinociceptive tolerance is, in part, the end results of a coordinated balance between processes governing desensitization and resensitization of MORs. Previous electrophysiological and biochemical studies have indicated that endogenous opioid peptides and certain nonpeptide agonists such as etorphine and fentanyl induce either functional desensitization or internalization of MORs. In contrast, morphine does not

promote detectable internalization of MORs in cultured cells after prolonged or acute treatment, although it is well established that morphine causes the development of antinociceptive tolerance in vivo [56]. Thus, the mechanisms underlying the development of tolerance to MOR agonists are still complicated. A potential limitation of our present understanding is that it is derived, in part, from multiple in vitro studies using several cell lines including the non-neural cell model. Therefore, in order to further understand properties of antinociceptive tolerance, I should investigate the utility of repeated treatment with MOR agonists at doses for the relief of the chronic pain associated with physiological change in endogenous MOR system and its related downstream signaling machinery.

The aim of the present study was then to investigate whether repeated administration of morphine or fentanyl could cause the development of tolerance to the morphine- or fentanyl-induced antinociceptive effects under the long-lasting pain-like state induced by intraplantar administration of CFA in mice. Additionally, I compared the effect of repeated administration of morphine or fentanyl on the regulatory process of MOR trafficking, which is responsible for receptor phosphorylation, internalization and recycling pathways following CFA injection in mice.

Materials and Methods

Animals

Male CXBK (The Jackson Laboratory, Bar Harbor, ME, USA and Tokyo Laboratory Animals Science Co., Tokyo, Japan), male C57BL/6J and ICR mice (Tokyo Laboratory Animals Science, Tokyo, Japan), weighing 22-30 g at the beginning of experiments, were housed in groups of 8-10 in a temperature-controlled room (23±1°C).

Drugs

The drugs used in the present study were morphine hydrochloride (Sankyo Co., Tokyo, Japan), fentanyl citrate (Hisamitsu Pharmaceutical Co., Tokyo, Japan) and CFA (Sigma Chemical Co., St. Louis, MO, USA). Morphine and fentanyl were dissolved in 0.9% saline.

Measurement of thermal hyperalgesia

To assess the sensitivity to thermal stimulation, each of the hind paws of mice was tested individually using a thermal stimulus apparatus (UGO-BASILE, Biological Research Apparatus, VA, Italy). The intensity of the thermal stimulus was adjusted to achieve an average baseline paw withdrawal latency of approximately 8 to 10 sec in naive mice. Only quick hind paw movements (with or without licking of the hind paws) away from the stimulus were considered to be a withdrawal response. Paw

movements associated with locomotion or weight shifting were not counted as a response. The paws were measured alternating between the left and right with an interval of more than 3 min between measurements. The latency of paw withdrawal after the thermal stimulus was determined as the average of three measurements per paw.

In the experiment of anti-hyperalgesic tolerance to opioids with repeated s.c. injection of morphine or fentanyl, mice were repeatedly injected with saline, morphine (3 mg/kg, s.c.) or fentanyl (30 μg/kg, s.c.) once a day for 15 consecutive days after saline or CFA injection. Measurement of thermal threshold was performed just before and 30 or 15 min after s.c. injection of saline, morphine or fentanyl on day 1, 7 and 15. Finally, % of reverse with standard error was calculated as $((T_1 - T_0)/(T_{day\ 0} - T_{day\ 1})) \times 100$, where T_0 and T_1 were thermal threshold before and after the s.c. injection of morphine or fentanyl on each test day and $T_{day\ 0}$ was thermal threshold before CFA-injection and $T_{day\ 1}$ was thermal threshold 1 day after CFA-injection.

Western blotting assay

The membrane fraction was prepared following the method described previously [57]. An aliquot of tissue sample was diluted with an equal volume of electrophoresis sample buffer (Protein Gel Loading Dye-2x; AMRESCO, Solon, OH, USA) containing 2% sodium dodecyl sulfate (SDS) and 10% glycerol with 0.2 M dithiothreitol. Proteins (10-20 μg/lane) were separated by size on 5-20% SDS-polyacrylamide gradient gel and transferred to a nitrocellulose membrane in a buffer containing 25 mM Tris and 192 mM

glycine. For immunoblot detection of protein kinase C γ (PKCγ), phosphorylated-PKC (activated form of PKC, p-PKC), G protein-coupled receptor kinase 2 (GRK2), phosphorylated-protein kinase A (activated form of PKA, p-PKA), phosphorylated-MOR (p-MOR, Ser 375), phosphorylated-protein phosphatase 2A (p-PP2A, Tyr 307) and Rab4, membranes were blocked in Tris-buffered saline (TBS) containing 0.3% nonfat dried milk (NAKARAI TESQUE, Inc., Kyoto, Japan) for 1 hr at room temperature with agitation. The membrane was incubated with primary antibody diluted in TBS containing 0.3% nonfat dried milk [1:1000 p-MOR (Cell Signaling Technology Inc., MA, USA), 1:2000 p-PP2A (Santa Cruz Biochemicals, Inc., CA, USA), 1:5000 Rab4 (Santa Cruz Biochemicals, Inc., CA, USA), 1:4000 PKCγ (Santa Cruz Biochemicals, Inc., CA, USA), 1:1000 p-PKC (Cell Signaling Technology Inc., MA, USA), 1:1500 GRK2 (Santa Cruz Biochemicals, Inc., CA, USA) and 1:1000 p-PKA (UPSTATE Inc., NY, USA)] overnight at 4 °C. The membranes were washed in Tween 20-TBS (TTBS) and then incubated for 2 hr at room temperature with horseradish peroxidase-conjugated goat anti-rabbit IgG (Southern Biotechnology Associates, Inc., Birmingham, AL, USA), which was diluted 1:10,000 in TBS containing 5% nonfat dried milk. After this incubation, the membranes were washed in TTBS. The antigen-antibody-peroxidase complex was then finally detected by enhanced chemiluminescence (PIERCE, Rockford, IL, USA) and visualized by exposure to Amersham Hyperfilm (Amersham Life Sciences, Arlington Heights, IL, USA). Film autoradiograms were analyzed and quantified by computer-assisted densitometry using NIH Image.

Statistical data analysis

The data are expressed as the mean with standard error of the mean (S.E.M.). The 50% effective concentration (EC_{50}) and 50% inhibitory concentration (IC_{50}) was calculated by GraphPad Prism Programs version 3.0 (GraphPad Software Inc., CA, USA). The statistical significance of differences between the groups was assessed by one-way or two-way analysis of variance (ANOVA), followed by the Bonferroni test or Student's *t*-test.

Results

Effect of single or repeated s.c. injection of morphine or fentanyl on thermal hyperalgesia induced by intraplantar injection of CFA in mice

Unilateral intraplantar injection of CFA into the mouse hind paw caused a marked decrease in the latency of paw withdrawal against a thermal stimulus only on the ipsilateral side in ICR mice (Fig. 1A and B). The persistent painful state caused by intraplantar injection of CFA lasted for more than 14 days following CFA treatment in mice (data not shown). The single s.c. injection of either morphine (1-10 mg/kg) or fentanyl (10-100 μg/kg) 1 day after CFA treatment recovered the decreased thermal threshold observed on the ipsilateral side in CFA-treated mice in a dose-dependent manner (Fig. 1A and B). At dose of 3.0 mg/kg or 30 μg/kg, s.c. administration of morphine or fentanyl, respectively, almost completely reversed the decrease in the thermal threshold without excessive effects in CFA-treated mice. Therefore, we proposed that the optimal doses for morphine- and fentanyl-induced anti-hyperalgesic effects in CFA-pretreated mice were 3.0 mg/kg and 30 μg/kg, respectively. As shown in figure 1C, the thermal hyperalgesia observed on the ipsilateral side after CFA injection was clearly reversed by each repeated s.c. injection of morphine (3 mg/kg) once a day for 15 consecutive days after CFA injection (Fig. 1C). On the contrary, the anti-hyperalgesic effect following the chronic treatment with fentanyl (30 μg/kg) was gradually tolerated (Fig. 1C).

Changes in levels of p-MOR, p-PP2A and Rab4 following repeated s.c. injection of

morphine or fentanyl in the spinal cord of CFA-pretreated mice

Western blots showed that the levels of p-MOR in the spinal cord were significantly increased following intraplantar administration of CFA compared to those in saline treated-mice ($p<0.01$; Fig. 2). Repeated s.c. administration of morphine induced a significant increase ($p<0.001$) in p-MOR levels in the spinal cord obtained from CFA-pretreated, but not saline-pretreated, mice compared to saline-saline treated group. On the other hand, the levels of p-MOR in the spinal cord were significantly increased following repeated s.c. treatment with fentanyl in either saline- or CFA-pretreated mice compared to those in saline-saline treated-group. As shown in figure 3, the immunoreactivities of PKCγ, p-PKC (activated form of PKC isoforms) , GRK2 and p-PKA (activated form of PKA) were not significantly different in the spinal cord of both saline- and CFA-pretreated mice following consecutive administration of morphine or fentanyl.

We next evaluated the effect of repeated s.c. treatment with morphine or fentanyl on the levels of p-PP2A, which is inactivated form of PP2A, in the spinal cord obtained from mice pretreated with CFA. As shown in figure 4A, we found that repeated s.c. treatment with fentanyl produced a significant increase in levels of p-PP2A in plasma membranes of the spinal cord obtained from CFA-, but not saline-, pretreated mice ($p<0.001$). In contrast, the level of p-PP2A following repeated injection of morphine in CFA-treated mice was similar to that in saline-treated mice.

As shown in figure 4B, s.c. treatment with fentanyl (30 μg/kg) produced a significant decrease in the expression of Rab4 in the spinal cord obtained from CFA-

pretreated, but not saline-pretreated, mice ($p<0.001$). In contrast, the same treatment with either saline or morphine failed to affect the expression of Rab4 in the spinal cord obtained from CFA-treated mice.

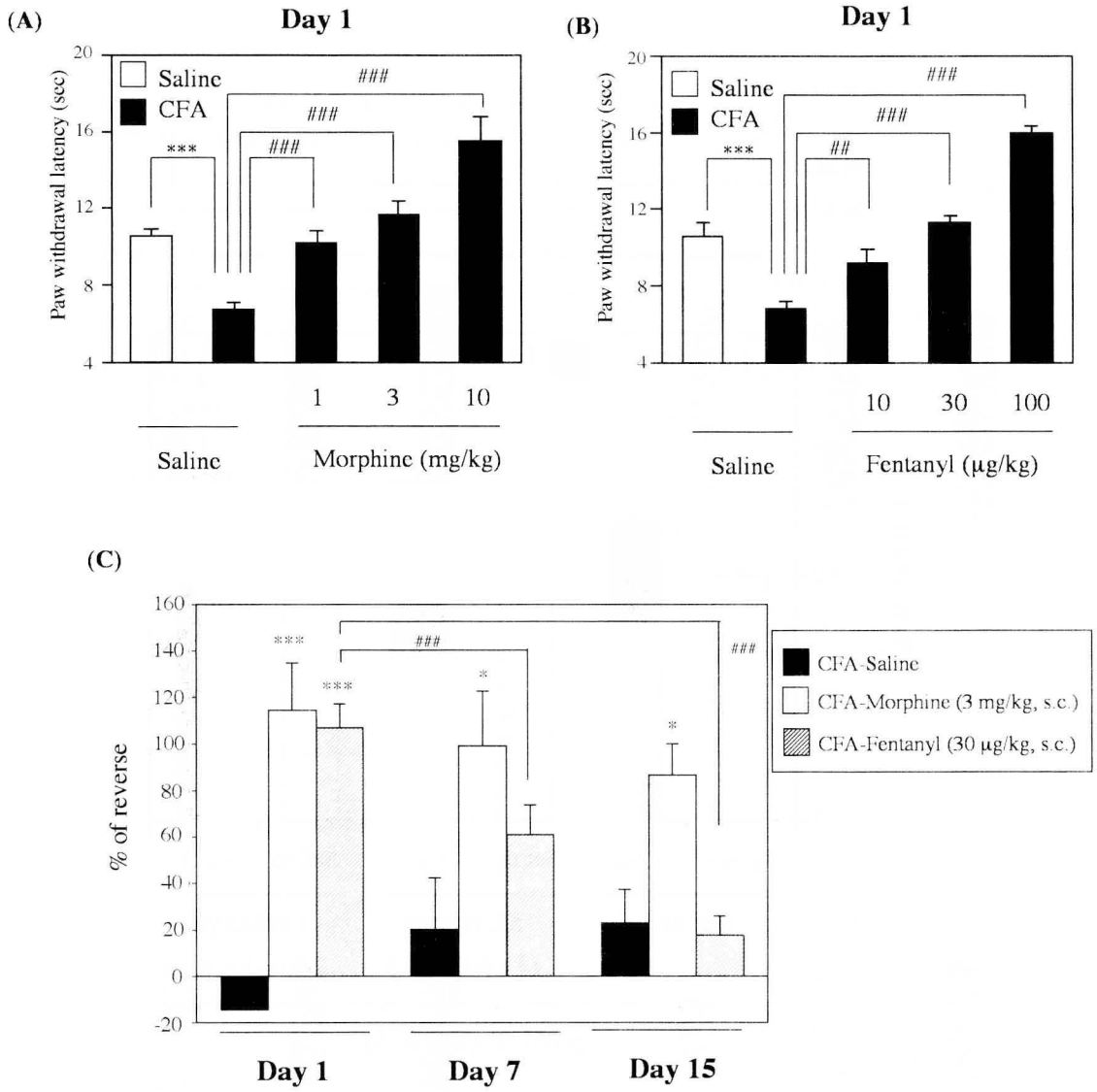

Fig. 1 Effect of s.c. injection of morphine or fentanyl on the latency of paw withdrawal in response to thermal stimulus on the ipsilateral side in saline- or complete Freund's adjuvant (CFA)-injected mice. Measurement of thermal threshold was performed just before and 30 or 15 min after s.c. injection of morphine or fentanyl, respectively. Groups of mice were treated s.c. with morphine (1-10 mg/kg) (A) or fentanyl (10-100 μg/kg) (B) 1 day after CFA injection. Each column represents the mean ± S.E.M. of 8-10 mice. ***$p<0.001$ vs. Saline-saline group, ##$p<0.01$ and ###$p<0.001$ vs. CFA-saline group. (C) Mice were repeatedly injected with saline, morphine (3 mg/kg) or fentanyl (30 μg/kg) once a day for 15 consecutive days after saline or CFA injection. Measurement of thermal threshold was performed 1, 7 and 15 days after CFA injection. Each point represents the mean ± S.E.M. of 8-10 mice. *$p<0.05$ and ***$p<0.001$ vs. CFA-saline group on each test day. ###$p<0.001$ vs. CFA-fentanyl group on day1.

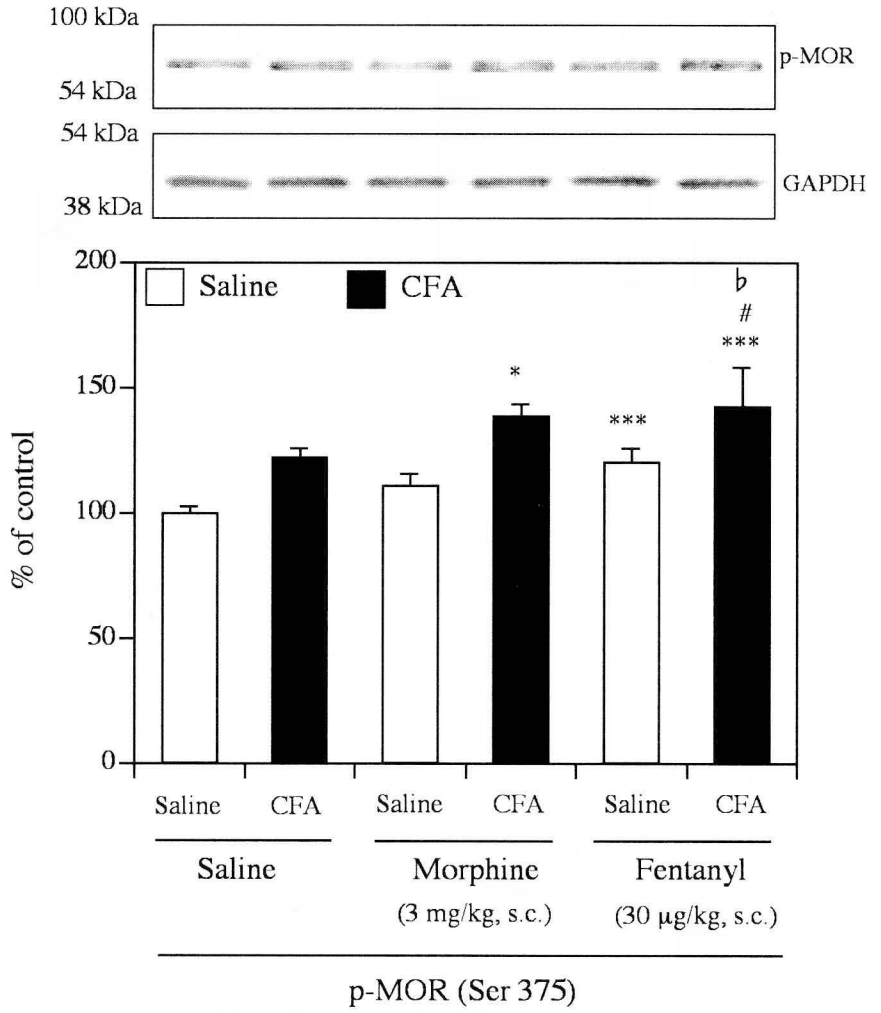

Fig. 2 Changes in levels of p-MOR (Ser 375) in membranes of the mouse spinal cord after repeated morphine (3 mg/kg) or fentanyl (30 μg/kg) treatment in saline- or CFA-injected mice. *Upper*: Representative Western blot for p-MOR. *Lower*: Change in the immunoreactivity for p-MOR in membranes of the spinal cord obtained from saline-, morphine- or fentanyl-treated mice with saline- or CFA-injection. Mice were repeatedly injected with saline, morphine (3 mg/kg) or fentanyl (30 μg/kg) once a day for 15 consecutive days following CFA injection. The membrane fraction was prepared at 24 hr after the last injection. Each column represents the mean ± S.E.M. of 3-6 independent samples. *$p<0.05$ and ***$p<0.001$ vs. Saline-saline group, #$p<0.05$ vs. CFA-saline group, ♭ $p<0.05$ vs. saline-fentanyl group.

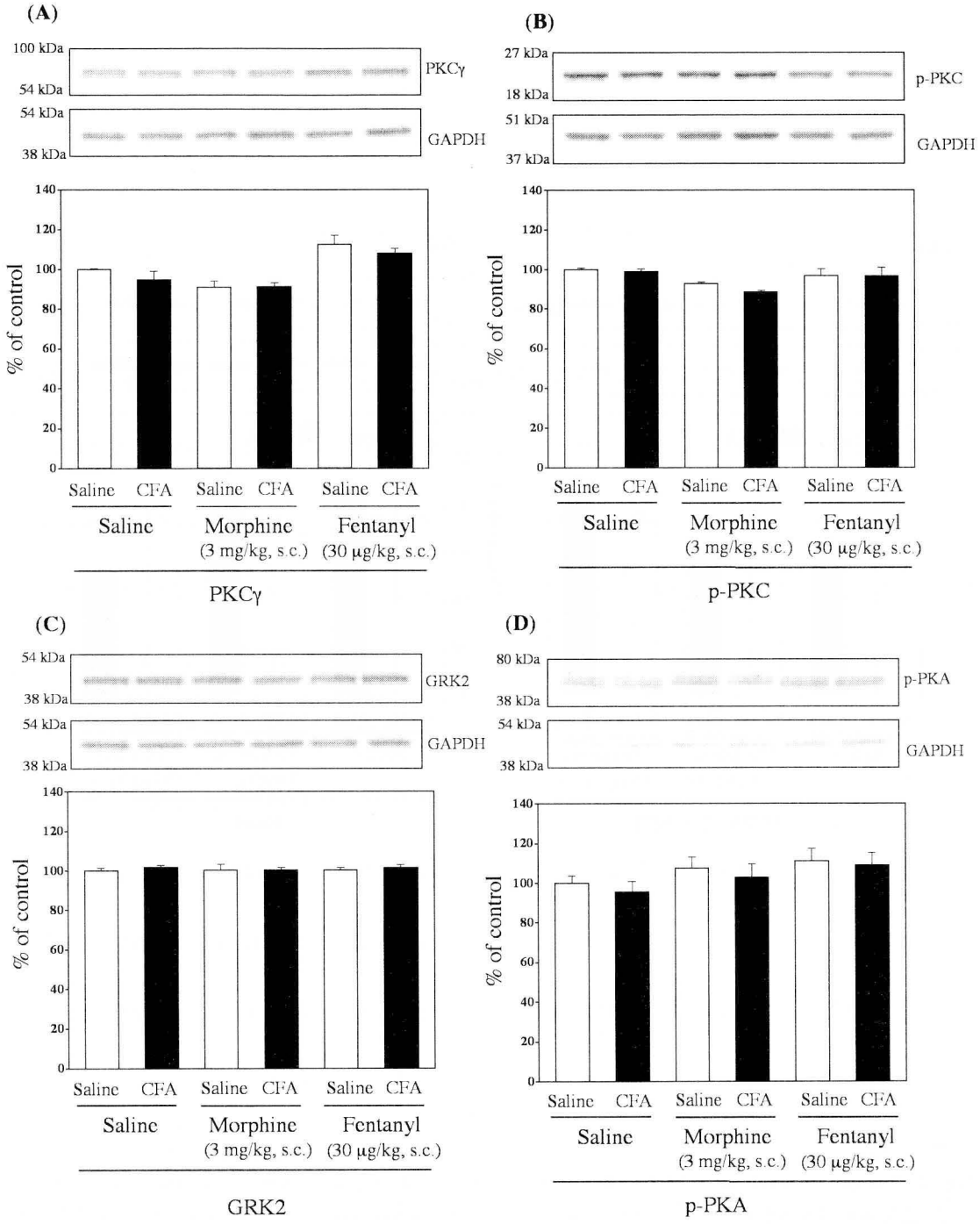

Fig. 3 Changes in levels of PKCγ (A), p-PKC (B), GRK2 (C) and p-PKA (D) in membranes of the mouse spinal cord after repeated morphine (3 mg/kg) or fentanyl (30 μg/kg) treatment in saline- or CFA-injected mice. *Upper*: Representative Western blot of each protein. *Lower*: Change in the immunoreactivity for each protein in membranes of the spinal cord obtained from saline-, morphine- or fentanyl-treated mice with saline- or CFA-injection. Mice were repeatedly injected with saline, morphine (3 mg/kg) or fentanyl (30 μg/kg) once a day for 15 consecutive days following CFA injection. The membrane fraction was prepared at 24 hr after the last injection. Each column represents the mean ± S.E.M. of 3-6 independent samples.

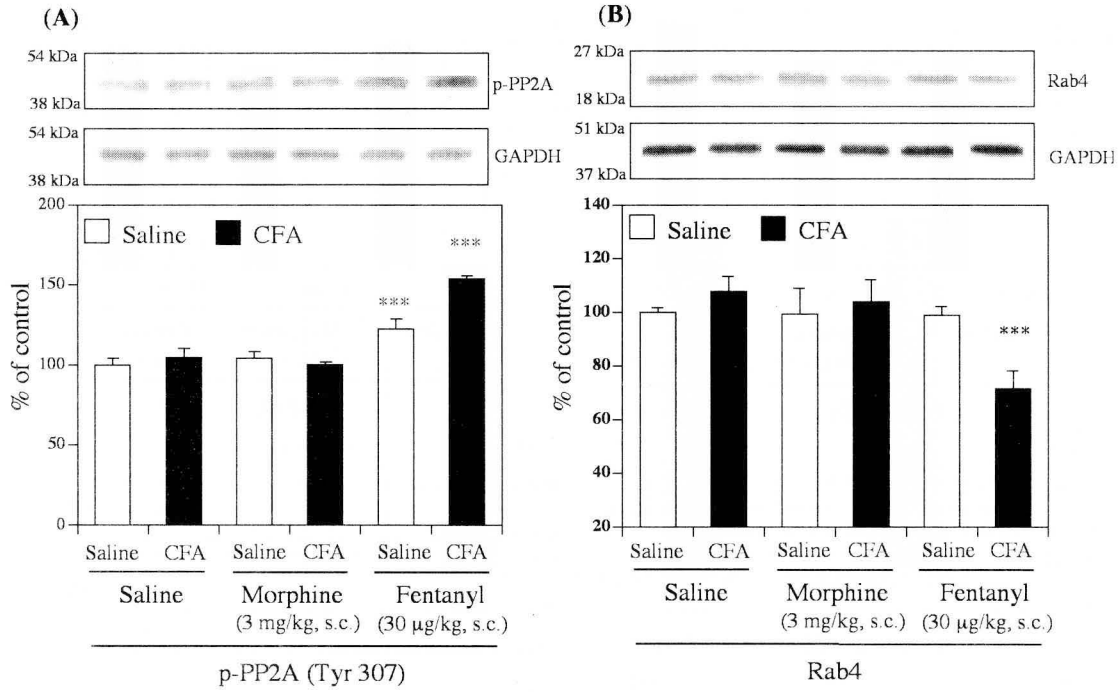

Fig. 4 Changes in levels of p-PP2A (Tyr307) (A) and Rab4 (B) in membranes of the mouse spinal cord after repeated morphine (3 mg/kg) or fentanyl (30 μg/kg) treatment in saline- or CFA-injected mice. *Upper*: Representative Western blot of each protein. *Lower*: Change in the immunoreactivity for each protein in membranes of the spinal cord obtained from saline-, morphine- or fentanyl-treated mice with saline- or CFA-injection. Mice were repeatedly injected with saline, morphine (3 mg/kg) or fentanyl (30 μg/kg) once a day for 15 consecutive days following CFA injection. The membrane fraction was prepared at 24 hr after the last injection. Each column represents the mean ± S.E.M. of 3-6 independent samples. (A) *** $p<0.001$ vs. Saline-saline group. (B) ***$p<0.001$ vs. Saline-saline group.

Discussion

In the present study, an inflammatory pain-like state induced by intraplantar injection of CFA was suppressed by s.c. treatment with either morphine or fentanyl in a dose-dependent manner. At dose of 3.0 mg/kg or 30 μg/kg, s.c. administration of morphine or fentanyl, respectively, completely reversed the decrease in the thermal threshold without excessive effects in CFA-treated mice. The key finding in the present study is that the anti-hyperalgesic effect induced by fentanyl in CFA-pretreated mice was rapidly disappeared during consecutive administration of fentanyl (30 μg/kg). On the contrary, morphine (3 mg/kg) preserved its potency of anti-hyperalgesic effect in CFA-pretreated mice even following repeated s.c. treatment with morphine. To our knowledge, these results are the first to indicate that the consecutive injection of fentanyl, unlike morphine, may extensively induce the development of tolerance to its anti-hyperalgesic effect under the persistent pain state.

A growing body of evidence suggests that the phosphorylation of MOR at diverse sites of its intracellular domain by GRK or second messenger-regulated protein kinases such as PKC and CaMKII has been shown to trigger the internalization of phosphorylated MOR from the cell surface to the cytosol [48]. These processes are thought to be an important step toward receptor desensitization. Among diverse serine/threonine residues of intracellular domain of MOR, phosphorylation of Ser 375 in the mouse MOR is essential for its internalization. In the present study, I found that the intraplantar injection of CFA resulted in an increase in levels of p-MOR (Ser 375) in

plasma membranes of the spinal cord. Consistent with this result, Narita et al. [39] previously reported that p-MOR-like-IR was clearly increased on the ipsilateral side in the superficial laminae of the L5 lumbar spinal dorsal horn under the long-lasting pain-like state induced by sciatic nerve ligation. A number of previous reports suggest that either PKCγ, GRK2 or PKA can be directly activated in response to the stimulation of MOR [58-60]. Subsequently, it is considered that activated PKCγ and GRK2 phosphorylate Ser 375 in the mouse MOR [48]. However, Western-blot analysis revealed no significant differences in levels of PKCγ, p-PKC, GRK2 and p-PKA in the spinal cord between saline- and CFA-pretreated mice following consecutive administration of morphine or fentanyl. It is of interest to note that repeated s.c. treatment with fentanyl further increased the protein level of p-MOR (Ser 375) in plasma membranes of the spinal cord under the inflammatory pain-like state. In contrast, the same treatment with morphine failed to affect the protein level of p-MOR (Ser 375) in the spinal cord. These results suggest that repeated injection of fentanyl, but not morphine, may markedly facilitate the phosphorylation of MOR in CFA-pretreated mice compared to that in saline-pretreated mice. After phosphorylation of Ser/Thr residues of the C-terminus, MORs are mostly internalized via clathrin-coated pits into early endosomes and subsequently dephosphorylated by intracellular protein phosphatases, such as PP2A [61]. The dephosphorylated MORs might be either recycled through sorting endosomes back to the plasma membrane or transported to the lysosomes for degradation. Here I also found that the protein level of p-PP2A (Tyr 307), which is the inactivated form of PP2A, in plasma membranes of the spinal cord

obtained from CFA-injected mice was significantly increased by repeated treatment with fentanyl, but not morphine. These findings point out the possibility that chronic pain may cause the different modulation on the process of the opioid receptor turnover between chronic morphine and fentanyl treatments. This hypothesis can be supported by the present immunoblotting studies examining the changes in levels of Rab4, which is the one of Rab GTPase, in the spinal cord of mice with chronic opioid treatment following CFA injection. Rab GTPase with over 60 members regulate intracellular vesicular membrane transport and membrane fusion events. Generally, it has been widely accepted that Rab4 localizes on the endocytic vesicle and participates in recycling process of receptor protein from early endosomes to the plasma membrane [65]. In the present study, the protein level of Rab4 in plasma membranes of the spinal cord obtained from CFA-injected mice was dramatically decreased by repeated treatment with fentanyl. On the contrary, the protein level of Rab4 following repeated injection of morphine in CFA-treated mice was similar to that in saline-treated mice. These results suggest that repeated treatment with fentanyl under the inflammatory pain state may lead to the facilitation of MOR phosphorylation/internalization and the attenuation of sorting internalized MOR back to the plasma membrane, whereas morphine does not cause such an event. The induction of MOR phosphorylation/internalization and the inhibiting MOR resensitization following the consecutive injection of fentanyl under the inflammatory pain state may directly contribute to the development of tolerance to fentanyl-induced antinociception in mice with CFA injection.

In conclusion, I demonstrated here that repeated treatment with fentanyl causes a

rapid desensitization to its anti-hyperalgesic effect under the inflammatory pain state, whereas morphine does not produce this phenomenon. Repeated treatment with fentanyl, but not morphine, results in the increase in levels of p-MOR associated with the enhanced inactivation of PP2A and the reduction in Rab4-dependent MOR resensitization. Although further experiments are still needed, this phenomenon provides the first evidence for the mechanism underlying the development of tolerance to fentanyl-induced antinociception under chronic pain-like sate.

Chapter 2

Reduced expression of a novel MOR subtype MOR-1B in CXBK mice: Implications of MOR-1B in the expression of MOR-mediated responses

Introduction

The MOR serves as the principle physiological target for the most clinically important opioid analgesics, including those with high addiction liability. It has been shown that MOR, as well as other opioid receptors, transduces signals through pertussis toxin (PTX)-sensitive Gi/Go proteins to inhibit adenylate cyclase, increase membrane K^+ conductance and reduce Ca^{2+} current [63].

The main two MOR subtypes, μ_1 and μ_2, have been proposed by a variety of receptor binding and pharmacological studies [64,65]. The naloxonazine-sensitive μ_1-receptor subtype is thought to play an important role in supraspinal analgesia, whereas the naloxonazine-insensitive μ_2-receptor subtype mediates spinal analgesia, respiratory depression and inhibition of gastrointestinal transit [66,67].

Many GPCR genes contain introns, which introduce the possibility of variants due to alternative splicing. Variations in gene-product splicing occur at the level of processing of heteronuclear-RNAs in the cell nucleus. A growing body of evidence suggests that alternative splicing with 14 exons results in several spliced variants for the cloned MOR [19, 20]. Several splice variant-dependent MOR subtypes that are different in length and amino acid composition only at the intracellular carboxyl terminus have been identified. Among the isolated variants, MOR-1 that has exon 1, 2, 3 and 4, and MOR-1B that contains an alternatively spliced exon 5 instead of the original exon 4, retain unique biochemical profiles [21,22]. Following agonist stimulation, MOR-1B shows an accelerated cycle of receptor endocytosis and reactivation, which in turn

promotes a greater resistance to agonist-induced desensitization than MOR-1 [21-23]. It should be mentioned that the MOR gene-targeted studies using mice with either a deletion of exon 1, 2 or 3 failed to distinguish the μ_1- and μ_2-receptor subtypes [68-71]. Although two subtypes may result from differential transcriptional modification, no report on the identification of μ_1 and μ_2 subtypes at the molecular level has been provided so far. It is of interest to note that a selective μ_1-receptor antagonist naloxonazine binds to MOR-1B as well as MOR-1, indicating the possibility that MOR-1B can encode μ_1-receptor subtype [21].

The CXBK mouse strain, which has been used in many studies to analyze the function of μ_1/μ_2 subtypes, is a recombinant-inbred strain derived by mating from a cross between C57BL/6J and BALB/c mice. This strain exhibits a significant lower levels of MOR in the brain area involving pain processing than those in its progenitor strains [72]. Autoradiographic studies have demonstrated that CXBK mice reveal a less density of the μ_1-receptor binding sites [72]. In the previous study, I demonstrated that the antinociceptive effect of intracerebroventricular (i.c.v.)-administered morphine or fentanyl, which was thought to be mediated by μ_1-receptor, was markedly reduced in CXBK mice [73]. The present study was then to investigate whether CXBK mice could be deficient in a putative splice variant-dependent MOR subtype.

Materials and Methods

Animals

Male CXBK and C57BL/6J mice (The Jackson Laboratory, Bar Harbor, ME, USA and Tokyo Laboratory Animals Science Co., Ltd., Tokyo, Japan), weighing 20-30 g at the beginning of experiments, were housed in groups of 8-12 in a temperature-controlled room. The animals were housed at a room temperature of 22 ± 1℃ with a 12 hr light-dark cycle (light on 8:00 am to 8:00 pm). Food and water were available *ad libitum.*

RNA preparation and semi-quantitative analysis by reverse transcription-polymerase chain reaction (RT-PCR)

Total RNA obtained from the mouse whole brain (except cerebellum) was extracted using the SV Total RNA Isolation system (Promega Co., Madison, WI, USA). First-strand cDNA was prepared as described [74] and the MOR gene was amplified in 50 μL of a PCR solution containing 0.8 mM $MgCl_2$, dNTP mix, and DNA polymerase with either synthesized primers of MOR-1 (sense: 5'-GCA TCC CAA CTT CCT CCA CAA TCG-3', antisense: 5'-CCA GGA AAC CAG AGC CTC CCA CAA-3') or MOR-1B (sense: 5'-CAA AAT ACA GGC AGG GGT CCA-3', antisense: 5'-AAT ACT ATT TTC TGG TGG TTA GTT C-3'). Samples were heated to 94℃ for 2 min, 55℃ for 2 min, and 72℃ for 3 min and cycled 39 times through 94℃ for 1 min, 55℃ for 2 min, and 72℃ for 3 min. The final incubation was at 72℃ for 7 min. The mixture was subjected

to 1% agarose gel that for electrophoresis with the indicated markers and primers for the internal standard β_2-microglobulin (β_2-MG). Each sample was applied more than two lanes in the same gel. The agarose gel was stained with ethidium bromide and photographed with UV transillumination. The intensity of the bands was analyzed and quantified by computer-assisted densitometry using an NIH image. For the control, the different intensities of each band provided from the sample of C57BL/6J mice were analyzed, and the average intensity was calculated. Then, each control intensity was again compared with the average intensity to calculate the standard error. Under these conditions, each intensity of bonds for the sample obtained from CXBK mice was analyzed and compared with the average intensity of that from C57BL/6J mice. Finally, % of control with standard error for the sample of CXBK mice was quantified with a computer-assisted imaging analysis system (NIH Image).

Immunohistochemistry

Mice were anesthetized with sodium pentobarbital (70 mg/kg, i.p.) and perfusion-fixed with 4% paraformaldehyde, pH 7.4. Then, the brains were removed quickly after perfusion and thick coronal section of the midbrain including periaqueductal gray matter (PAG) region was initially dissected using Brain Blocker (Neuroscience Inc., Tokyo, Japan). The coronal section of the midbrain was post-fixed in 4% paraformaldehyde for 2 hr. After the brains were permeated with 20% sucrose for 2 days and 30% sucrose for 2 days, they were frozen in an embedding compound (Sakura Finetechnical Co., Tokyo, Japan) on isopentane using liquid nitrogen and stored at -30

°C until used. Frozen 10 μm-thick coronal sections were cut with a cryostat (Leica CM1510; Leica Microsystems, Heidelberg, Germany) and thaw-mounted on poly-L-lysine-coated glass slides. The brain sections were blocked in 10% normal horse serum (NHS) in 0.01 M phosphate-buffered saline (PBS) for 1 hr at room temperature. Sections were incubated in primary antisera to MOR-1B (1:5000) (Gramsch Laboratories, Schwabhausen, Germany), which recognizes the amino acid sequence corresponding to the carboxyl-terminal of MOR1B (TVDRTNHQKIDLF), 2 overnight at 4℃. The antibody was then rinsed and incubated with each secondary antibody for 2 hr at room temperature. For the labeling, Alexa 488-conjugated goat anti-rabbit IgG for MOR-1B was diluted 1:400 in PBS containing 10% normal horse serum. In the present study, each slice obtained from CXBK or C57BL/6J mice were incubated on the same slides. The slides were then coverslipped with PermaFluor Aqueous mounting medium (Immunon; Thermo Shandon, Pittsburgh, PA). Fluorescence immunolabeling was detected using a U-MNIBA filter cube (Olympus, Tokyo, Japan) for Alexa 488. Digitized images of PAG sections were captured at a resolution of 1,316 x 1,035 pixels with camera. The density of MOR-1B labeling was measured with a computer-assisted imaging analysis system (NIH Image), according to the method described previously [78]. The upper and lower threshold density range were adjusted to encompass and match the immunoreactivity to provide an image with immunoreactive material appearing in black pixels, and non-immunoreactive material as white pixels. A standardized rectangle was positioned over the PAG area of C57BL/6J mice. The area and density of pixels within the threshold value representing immunoreactivity were calculated and the integrated

density was the product of the area and density. The same box was then 'dragged' to the corresponding position on the PAG area of CXBK mice and the integrated density of pixels within the same threshold was again calculated. The value for CXBK mice was expressed as percentage of control.

[^{35}S]GTPγS binding assay

For the membrane preparation, whole brain (except cerebellum) was removed from mice, and rapidly transferred to a tube filled with an ice-cold buffer. The membrane homogenate (3-8 μg protein/assay) was prepared as described [76] and incubated at 25℃ for 2 hr in 1 mL of assay buffer with various concentrations of endomorphin-1 (0.01-10 μM), 30 μM guanosine-5'-diphosphate (GDP) and 50 pM [^{35}S]GTPγS (specific activity, 1000 Ci/mmol; Japan Radioisotope Association, Tokyo, Japan). The reaction was terminated by the filtration using Whatman GF/B glass filters. The filters were washed three times and then transferred to scintillation-counting vials containing tissue solubilizer (Soluene-350; Packard Instrument Co., Meriden, CT, USA) and scintillation cocktail (Hionic Fluor; Packard Instrument Co., Meriden, CT, USA). The radioactivity in the samples was determined with a liquid scintillation analyzer. Non-specific binding was measured in the presence of 10 μM unlabeled GTPγS.

Assessment of antinociception

Antinociception was determined by the tail-flick test. The intensity of the heat stimulus was adjusted so that the animal flicked its tail after 3-5 sec. The inhibition of

this tail-flick response was expressed as a percentage of the maximum possible effect, which was calculated as $((T_1 - T_0)/(T_2 - T_0)) \times 100$, where T_0 and T_1 were the tail-flick latencies before and after the i.c.v. injection of endomorphin-1 (10, 17, 24 nmol/mouse) and T_2 was the cut-off time (set at 10 sec) in the tests to avoid injury to the tail. The antinociceptive effect of endomorphin-1 was measured at 10 min after i.c.v. injection.

Injection procedure

The i.c.v. administration was performed following the method described previously [77]. In order to make a hole in the skull for the injection, one day before the administration of antisense oligodeoxynucleotide, mismatch oligodeoxynucleotide or saline, mice were briefly anesthetized with ether and a 2-mm double-needle (tip: 27G× 2 mm and base: 22G×10 mm, Natsume Seisakusyo Co., Tokyo, Japan) attached to a 25-μL Hamilton microsyringe was inserted into the unilateral injection site. The unilateral injection site was approximately 2 mm from either side of the midline between the anterior roots of the ears. The head of the mouse was held against a V-shaped holder and the drugs were injected into the hole. The injection volume was 4 μL for each mouse. Each solution was injected without injection cannulae.

Administration of antisense oligodeoxynucleotide (AS-ODN) and endomorphin-1

Synthetic end-capped phosphorothioate AS-ODN and mismatch oligodeoxynucleotide (MM-ODN), corresponding to exon 5 in MOR-1B cDNA, were prepared. Sequences were as follows: AS-ODN, 5'-AAA TAA TAC TAT TTT-3' and

MM-ODN , 5'-TAA AAA TCA TTT TAT-3'. C57BL/6J mice were received with saline (4 μL/mouse/day), AS-ODN (5 μg/mouse/day) or MM-ODN (5 μg/mouse/day) injected i.c.v. into the unilateral ventricle. Single i.c.v. injection of each oligodeoxynecleotide or saline was performed once daily for 3 days based on the schedule described previously: i.e. days1, 2 and 3. An interval of 24 hr was selected between oligodeoxynecleotide administrations to minimize the neurotoxic damage. On day 4, a selective endogenous MOR agonist endomorphin-1 (10, 17 and 24 nmol/mouse) was injected into the same hole of lateral cerebral ventricle with a 25-μL Hamilton microsyringe and the antinociceptive effect induced by endomorphin-1 was evaluated by the tail-flick test at 10 min after i.c.v. injection.

Statistical data analysis

The data are expressed as the mean with S.E.M. The statistical significance of differences between the groups was assessed by one-way or two-way ANOVA, followed by the Bonferroni/Dunn multiple comparison test.

Results

Reduction in the expression of MOR-1B mRNA in the supraspinal site of CXBK mice as compared to that in their progenitor C57BL/6J mice

To investigate the expression of spliced-variant dependent MOR subtypes MOR-1 and MOR-1B mRNAs in the whole brain of CXBK mice, I carried out semi-quantitative analysis of MOR-1 and MOR-1B mRNAs using RT-PCR assay. The expression of either MOR-1 or MOR-1B mRNA can be observed in the whole brain obtained from C57BL/6J mice. A single band migrating at 245 and 547 bp was detected for MOR-1 and MOR-1B mRNAs, respectively. In the present study, the level of MOR-1B mRNA was markedly lower in CXBK mice than that in C57BL/6J mice ($p<0.05$, Fig. 1). In contrast, there was no significant difference in MOR-1 production between the two strains (Fig. 1).

Reduction in the level of MOR-1B-like immunoreactivity in the PAG region of CXBK mice as compared to that in their progenitor C57BL/6J mice

In the immunohistochemical study, MOR1B-IR was distributed in the PAG area in C57BL/6J mice (Fig. 2A). However, relatively less MOR-1B-IR was seen in the same subset of the PAG area of CXBK mice (Fig. 2B). A significant decrease in MOR-1B-IR was detected in the PAG region of CXBK as compared to that in C57BL/6J mice ($P<0.001$, Fig. 2C).

Comparison of supraspinal antinociceptive effect and G-protein activation induced by endomorphin-1 between CXBK and C57BL/6J mice

I next investigated whether CXBK mice could affect the G-protein activation by MOR agonists in membranes of the whole brain (Fig. 3A). The ability of a selective endogenous MOR ligand endomorphin-1 to activate G-proteins in the brain of C57BL/6J and CXBK mice was examined by monitoring the binding of [^{35}S]GTPγS to brain membranes. Endomorphin-1 (0.01-10 μM) produced a concentration-dependent increase in the binding of [^{35}S]GTPγS to whole brain membranes obtained from C57BL/6J mice. In contrast, the binding of [^{35}S]GTPγS stimulated by endomorphin-1 was significantly decreased in CXBK mice ($P<0.01$ or $P<0.001$ vs. C57BL/6J mice, Fig. 3A).

Additional evidence for the reduced MOR function in CXBK mice with respect to the antinociceptive response to endomorphin-1 was obtained in the tail-flick test. The i.c.v. administration of endomorphin-1 produced a profound antinociception in C57BL/6J mice. The CXBK mice were virtually devoid of the robust endomorphin-1-induced antinociception ($P<0.01$ or $P<0.001$ vs. C57BL/6J mice, Fig. 3B).

Effects of i.c.v. injection of AS-ODN targeting exon 5 of MOR gene on the expression of MOR-1B and endomorphin-1-induced antinociception in the supraspinal site

Finally, I examined whether the knockdown of MOR-1B expression by i.c.v. pretreatment with AS-ODN to exon 5 of MOR in the brain from C57BL/6J mice could

influence the antinociceptive effect of endomorphin-1. The level of MOR-1B mRNA was detectable in the whole brain obtained from C57BL/6J mice treated i.c.v. with either saline or the MM-ODN to exon 5 of MOR with the same degree, whereas i.c.v. treatment with AS-ODN to exon 5 of MOR produced a significant decrease in MOR-1B mRNA levels ($p<0.05$ vs. saline, Fig. 4A, B). In contrast, the same treatment produced no significant difference in levels of MOR-1 expression (Fig. 4A, B). Under these conditions, the dose-response lines for the endomorphin-1-induced antinociception in C57BL/6J mice pretreated with either saline or the MM-ODN to exon 5 of MOR were markedly shift to the right by pretreatment with AS-ODN to exon 5 of MOR ($P<0.01$ or $P<0.001$ vs. saline or MM-ODN, Fig. 4C), being in good agreement with the findings in CXBK mice (shown in Fig. 3B).

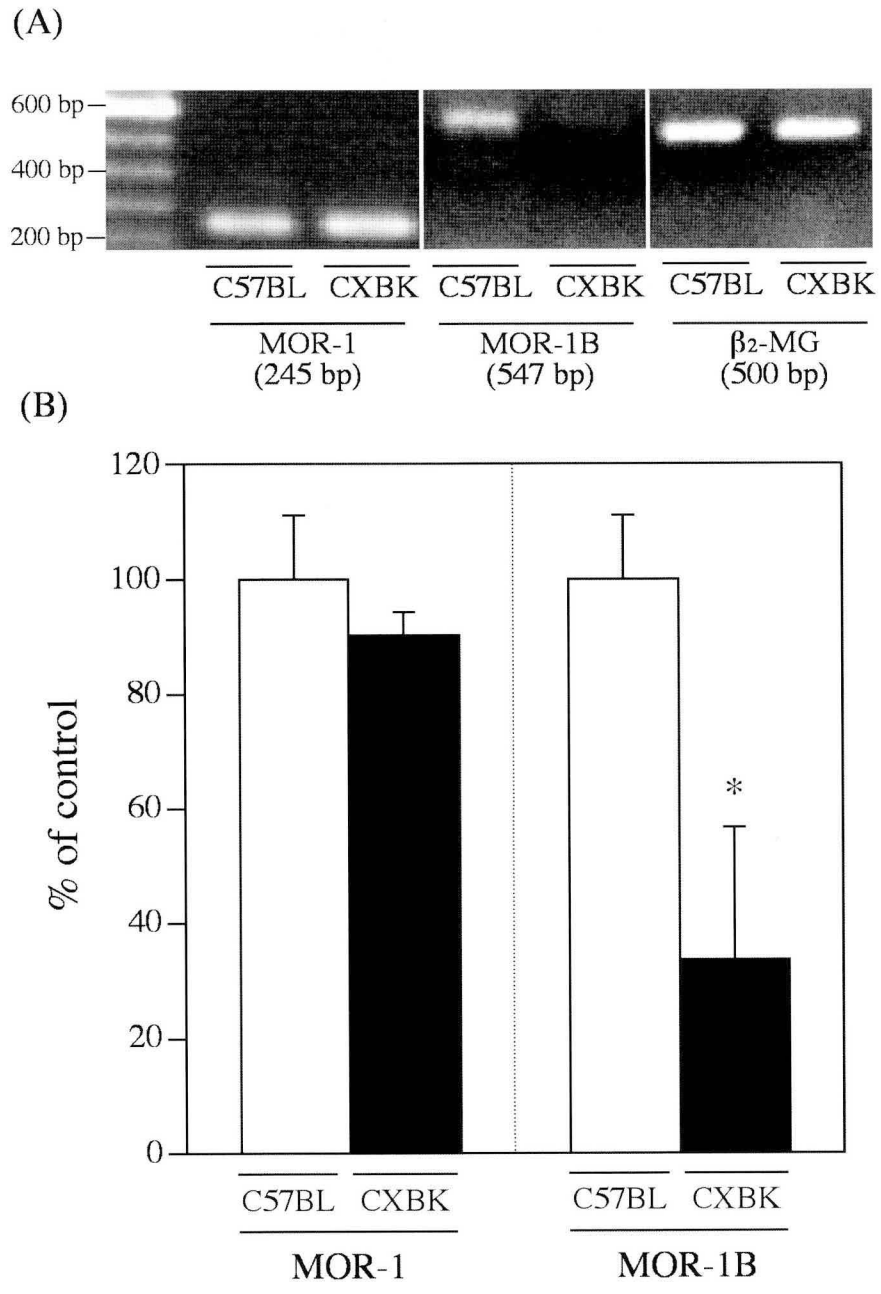

Fig. 1 Reduced expression of MOR-1B mRNA in the whole brain of CXBK mice. (A) Representative RT-PCR for MOR-1 and MOR-1B mRNAs in the brain obtained from C57BL/6J (C57BL) and CXBK mice. The sample mixture was subjected to 1% agarose gel electrophoresis with the indicated markers and primers for the internal standard β_2-MG. Six experiments using three independent samples were performed in this study. (B) Semi-quantitation of the intensity of the bands. The value for CXBK mice is expressed as a percentage against C57BL mice. Each column represents the mean ± S.E.M. of six experiments. *$p<0.05$ vs. C57BL mice.

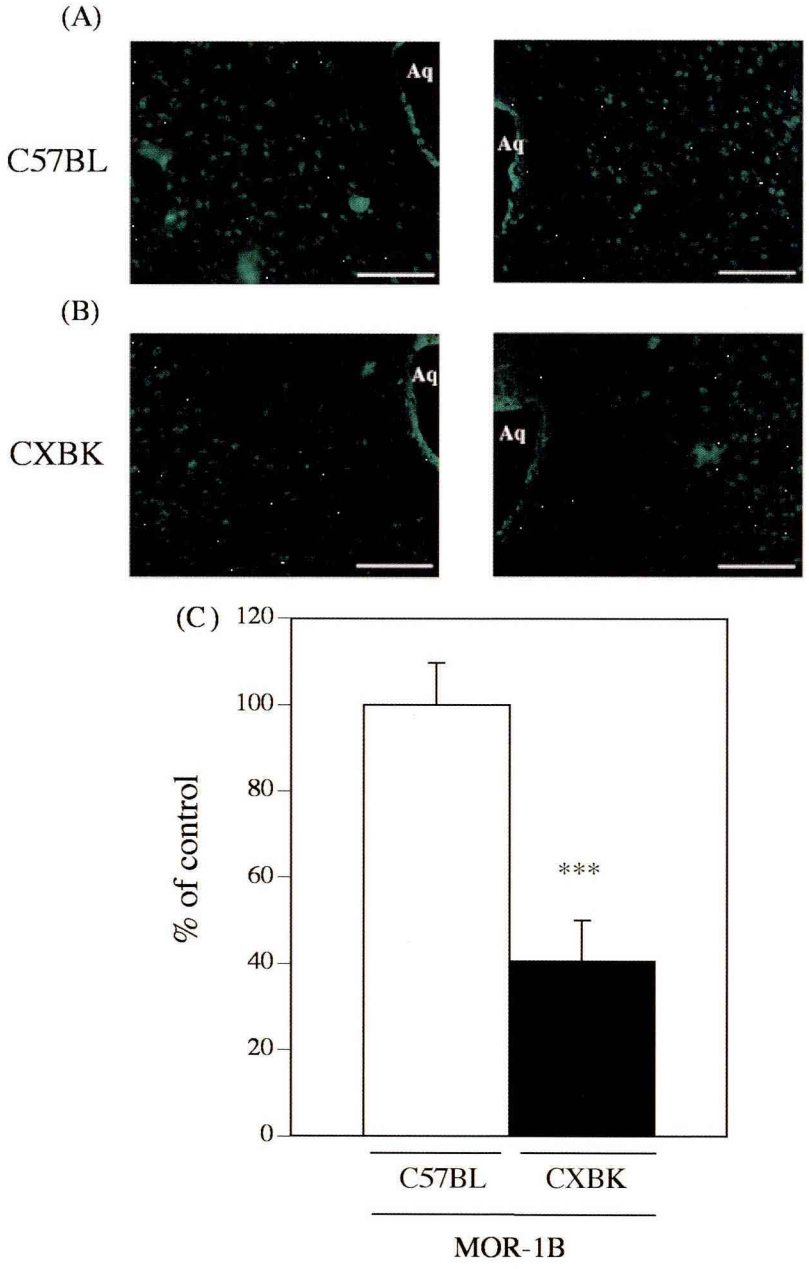

Fig. 2 Reduced MOR1B-like immunoreactivity (MOR1B-IR) in the PAG of CXBK mice. Coronal sections including the PAG were obtained from C57BL/6J (C57BL) (A) and CXBK mice (B). The decreased MOR1B-IR was detected in the PAG of CXBK mice. Scale bars = 50 μm. (C) Semi-quantitative analysis of MOR-1B-IR in the PAG area of C57BL and CXBK mice. The value for CXBK mice is expressed as a percentage of the density against C57BL mice. Each column represents the mean ± S.E.M. of six experiments.

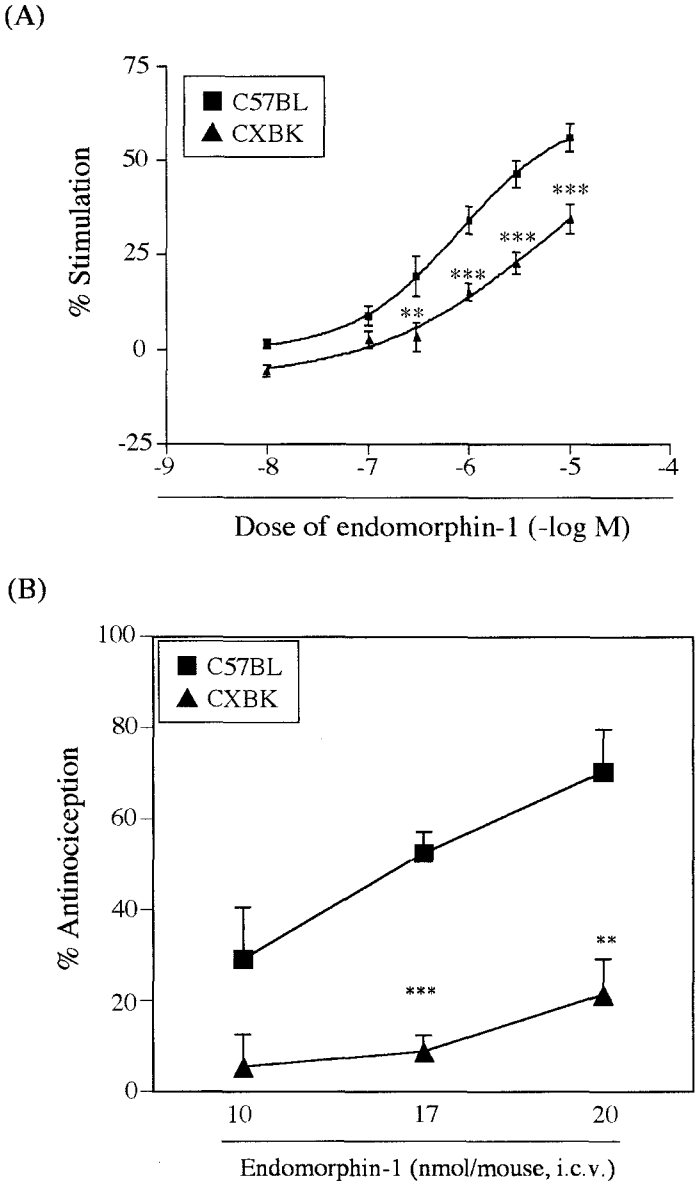

Fig. 3 Effect of an endogenous MOR ligand endomorphin-1 on the binding of [^{35}S]GTPγS to membranes of the whole brain obtained from C57BL/6J (C57BL) and CXBK mice. Membranes were incubated with 50 pM [^{35}S]GTPγS and 30 μM GDP with or without different concentrations (0.01-10 μM) of endomorphin-1 for 2 hr at 25℃. The data are expressed as a percentage of basal [^{35}S]GTPγS binding measured in the presence of GDP and absence of agonist. The data represent the mean ± S.E.M., at least, of three independent experiments. **p<0.01, ***p<0.001 vs. C57BL mice. The F value of two-way ANOVA in endomorphin-1 is F(1, 56)=60.77. (B) Dose-response lines for the antinociceptive effect produced by i.c.v. administration of endomorphin-1 in C57BL/6 and CXBK mice using a tail-flick assay. Tail-flick latencies were measured at 10 min after i.c.v. injection of endomorphin-1 (10-24 nmol/mouse). Antinociception was expressed as a percentage of the maximal possible effect (% Antinociception). The data represent the mean ± S.E.M. of 6-8 mice. **p<0.01, ***p<0.001 vs. C57BL mice.

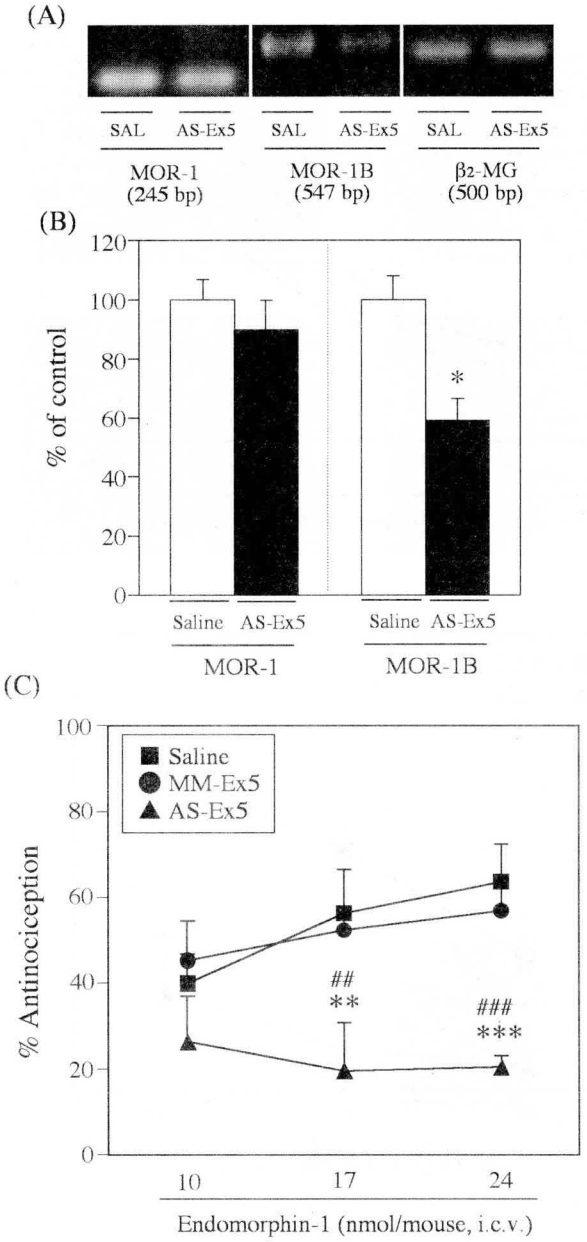

Fig. 4 (A) Representative RT-PCR for MOR-1 and MOR-1B mRNAs in the brain obtained from C57BL/6 mice following treatment with saline or antisense oligodeoxynucleotide against exon 5 of MOR (AS-Ex5). An i.c.v. pretreatment with saline, AS-Ex5 (5 μg/mouse) and mismatch oligodeoxynucleotide (MM-Ex5, 5 μg/mouse) against exon 5 of MOR were performed once a day for 3 days. On day 4, the samples for RT-PCR were obtained from each group. The sample mixture was subjected to 1% agarose gel electrophoresis with the indicated markers and primers for the internal standard β_2-MG. Six experiments using three independent samples were performed in this study. (B) Semi-quantitation of the intensity of the bands. The value for mice pretreated with AS-Ex5 is expressed as a percentage of the increase in mice pretreatment with saline. Each column represents the mean ± S.E.M. of six experiments. *$p<0.05$ vs. saline group. (C) Effect of AS-Ex5 on the endomorphin-1-induced antinociception in C57BL/6J mice. The data represent the mean ± S.E.M. of 6-8 mice. **$p<0.01$, ***$p<0.001$ vs. saline groups. ##$p<0.01$ vs. MM-Ex5 group.

Discussion

In the present study, I demonstrated for the first time that CXBK mice display a significant reduction in the expression of MOR-1B mRNA in the brain as compared to that in their progenitor C57BL/6J mice. In contrast, the expression level of MOR-1 mRNA in the brain of CXBK mice was similar to that found in C57BL/6J mice, indicating a specific loss of MOR-1B mRNA expression in this strain.

To further clarify whether CXBK mice could exhibit lower levels of MOR-1B protein in the brain, the immunohistochemical study was performed using the specific antibody to MOR-1B. In the PAG of CXBK mice, relatively lower levels of MOR-1B-IR were detected as compared to those observed in C57BL/6J mice. The present data indicate that the reduction in mRNA expression of MOR-1B in CXBK mice leads to a decrease in levels of MOR-1B protein in the PAG compared to those in C57BL/6J mice. Such findings strongly support my hypothesis that CXBK strain can be classified as MOR-1B-knockdown mice.

Since CXBK mice had a lower level of MOR-1B expression in the PAG than that observed in C57BL/6J, I next examined whether a significant deficiency of MOR-1B in CXBK mice could affect the MOR function to activate G-proteins. As I expected, the increase in [^{35}S]GTPγS binding to whole brain membranes induced by a selective MOR agonist endomorphin-1 in C57BL/6J mice was significantly decreased in CXBK mice. These results suggest that a less ability to stimulate G-protein via MOR in CXBK mice may result from the decreased level of MOR-1B expression.

It has been reported that alternative splicing with ten to twelve exons results in seven or more spliced variant for the cloned MOR (ex. MOR1 and MOR1A-MOR1F). Previous immunohistochemical study demonstrated that MOR-1-IR is found abundantly in the striatum, whereas no MOR-1C-IR is detected in the same region [25]. Furthermore, MOR-1C, but not MOR-1, are distributed in the superficial laminae of the dorsal horn, and involved in presynaptic inhibition of transmitter release from peptide-containing afferents to the dorsal horn [26]. Considering these findings, it can be speculated that each splice variants derived from the same MOR gene reveals a differential distribution in the CNS and regulates individual physiological and pharmacological function. In term of MOR1B, although there are increasing evidences that MOR-1B regulates some biochemical functions including receptor trafficking [22], the inhibition of forskolin-induced cAMP accumulation [21] and the increase in intracellular Ca^{2+} concentration resulting from the stimulation of inositol trisphosphate formation [78], the role of MOR-1B in behavioral effects of MOR agonists was not fully understood. In the present study, I found that i.c.v. treatment with AS-ODN to exon 5 of MOR produced a specific reduction in the expression of MOR-1B mRNA, and a significant suppression of the i.c.v.-administered endomorphin-1-induced antinociception. Furthermore, MOR-1B-knockdown CXBK mice showed reduced antinociceptive effect of endomorphin-1 as compared to that in C57BL/6J mice. These findings strongly suggest that MOR-1B may be the primary site for the expression of supraspinal antinociception induced by MOR agonists.

High density of μ_1-receptor binding site has been observed in the PAG, medial

thalamus and medial raphe, which are considered to be critical sites to regulate the antinociception of MOR agonists, in rodents [18,50]. Especially, the PAG is the major site involved in the modulation of nociceptive input, through desending inhibitory serotonergic neurons that project to the spinal cord. Generally, it is considered that the facilitation of desending systems is modulated by inhibition of γ-aminobutyric acid (GABA)-containing interneuron. Activation of central MOR may lead to the inhibition of GABA release, resulting in the stimulation of the desending pathway. In the present study, I found that MOR-1B-IR was prominently expressed and detected in the PAG of C57BL/6J mice. The finding is inconsistent with the previous report by Schulz et al that MOR-1B appears to be predominantly localized to the olfactory bulb in the rat. Conversely, it was reported that the expression of MOR-1B mRNA can be observed in many brain areas. The highest concentrations of MOR-1B mRNA are detected in the frontal cortex and the striatum, and the lowest concentrations are found in the olfactory bulb and the cerebellum [21]. In this point, I found here that, like MOR-1 mRNA, MOR-1B mRNA is detectable in the whole brain tissue obtained from C57BL/6J mice. Although the specific reason for these discrepancies between previous immnohistochemical studies and our studies remains unclear, one possibility is that the discrepancy may result from species differences or different experimental conditions. Receptor autoradiographic study has demonstrated that the CXBK strain is deficient in μ_1-receptor binding site in several brain regions associated with pain regulation [72]. It should be pointed out that i.c.v. pretreatment with an AS-ODN probe targeting the coding region of exon 5 of MOR gene suppressed supraspinal antinociception by

endomorphin-1, which is known to be reversed by a μ_1-receptor antagonist naloxonazine [79]. Although further experiments are needed to perform, it is likely that the μ_1-receptor is closely related to the MOR-1B.

In conclusion, the present study provides new insights into the mechanism underlying the reduced antinociceptive response to MOR agonists in CXBK mice. Furthermore, I propose here that a MOR gene-derived alternative splice variant, MOR-1B may be a candidate to express a less activity of MOR agonists in the CXBK phenotype, and play an important role in supraspinal antinociception of MOR agonists.

Chapter 3

The specific involvement of the opioid receptor types and MOR subtypes in antinociceptive properties of morphine and fentanyl

Introduction

According to the WHO guidelines for patients with moderate or severe pain, a typical MOR agonist morphine has been a "gold standard" for treatment of moderate to severe cancer pain. The intrathecal administration of morphine has been the standard therapy to control long-term intractable pain. However, the use of morphine is sometimes accompanied by side effects such as emesis and constipation [40,41]. In 1959, fentanyl, the anilidopiperidine class of MOR agonist, was reported as a potent synthetic analgesic with a lower propensity to produce these undesirable effects in the clinical setting. The low molecular weight and lipid solubility of fentanyl make it possible for delivery via the transdermal therapeutic system. To date, a number of studies concerning differences of the antinociceptive property between morphine and fentanyl have been undertaken. It has been well established that fentanyl has a high affinity for MORs and exhibits 50-100 times more potent analgesic activity than that of morphine [42]. In addition, as mentioned in Chapter 1, I demonstrated that the anti-hyperalgesic effect induced by fentanyl in CFA-pretreated mice was rapidly disappeared during consecutive administration of fentanyl, whereas morphine preserved its potency of anti-hyperalgesic effect in CFA-pretreated mice even following repeated s.c. treatment with morphine. However, the certain mechanisms underlying antinociception induced by each MOR agonist are not fully understood. It is likely that the reason for the limited application of morphine or fentanyl in the clinical setting is related to a poor understanding the difference of certain mechanisms underlying the antinociceptive

effects of these MOR agonists.

Several genetic mouse models of differential sensitivity to opioids have been used to investigate the mechanisms underlying individual variation in responses to opioids. Among a number of mouse models, the CXBK mouse strain has been used in many studies to analyze the functional role of MOR subtypes in the CNS. It has been widely accepted that CXBK mice are recombinant inbred mice derived by full-sib mating from a cross between the C57BL/6J and BALB/cJ strains. CXBK mice have a partial deficiency of MOR [52], and the level of MOR mRNA in the brain of CXBK mice is reduced to approximately 60% of their progenitor mice [55]. As shown in Chapter 2, I found that CXBK strain can be classified as supraspinal MOR-1B-knockdown mice, and MOR-1B plays an important role in supraspinal antinociception of the endogenous MOR agonist endomorphin-1. It is therefore worthwhile to use CXBK mice to further investigate the mechanisms underlying the antinociceptive effects induced by MOR agonists such as morphine and fentanyl.

Thus, the goal of the present study was to clarify the analgesic properties of morphine and fentanyl in the mouse supraspinal and spinal cord. I investigated the effects of pretreatment with MOR, DOR and KOR antagonists, β-FNA, NTI and nor-BNI, respectively, on the antinociceptive effect induced by morphine or fentanyl using the mouse tail-flick test. In addition, I compared ED_{50} values for antinociceptive effects between morphine and fentanyl at peripheral, spinal and supraspinal site, respectively in ICR mice. Finally, I tired to investigate the specific involvement of MOR subtypes at either the spinal or supraspinal site in antinociceptive properties of

morphine and fentanyl using CXBK mice.

Materials and Methods

Animals

Male ddY (20-30 g), male ICR (20-30 g), male CXBK (20-30 g) and C57BL/6J (20-30 g) mice were obtained from Tokyo Laboratory Animals Science Co. (Tokyo, Japan). The animals were housed at a room temperature of 22 ± 1 °C with a 12 hr light-dark cycle (light on 8:30 a.m. to 8:30 p.m.), and were allowed to adapt to this environment for 3 days before the experiments. Food and water were available *ad libitum.*

Drugs

The drugs used in the present study were fentanyl citrate (Hisamitsu Pharmaceutical Co., Tokyo, Japan), morphine hydrochloride (Sankyo Co., Tokyo, Japan), β-FNA, NTI, cyclic-[D-Pen^2, D-Pen^5] enkephalin (DPDPE), nor-BNI and trans-3,4-dichloro-N-(2-(1-pyrrolidinyl)-cyclohexyl)benzene-acetamide (U-50,488H) (Toray Industries, Kanagawa, Japan) and CFA (Sigma Chemical Co., St. Louis, MO, USA). β-FNA (40 mg/kg), naloxonazine (35 mg/kg), NTI (3 mg/kg) and nor-BNI (3 mg/kg) were administered s.c. 24 hr, 24 hr, 30 min and 4 hr, respectively, before morphine or fentanyl injection. All opioid agonists and antagonists were dissolved in saline.

RNA preparation and semi-quantitative analysis by RT-PCR

Total RNA obtained from the spinal cord of CXBK or C57BL/6J mice was extracted using the SV Total RNA Isolation system (Promega Co., Madison, WI, USA).

First-strand cDNA was prepared as described previously by Narita et al. [74] and the MOR gene was amplified in 50 μL of a PCR solution containing 0.8 mM $MgCl_2$, dNTP mix, and DNA polymerase with either synthesized primers of MOR (sense: 5'-AGA CTG CCA ACC AAC ATC TAC AT-3', antisense: 5'-TGG ACC CCT GCC TGA TAT TTT G-3'), MOR-1 (sense: 5'-GCA TCC CAA CTT CCT CCA CAA TCG-3', antisense: 5'-CCA GGA AAC CAG AGC CTC CCA CAA-3') or MOR-1B (sense: 5'-CAA AAT ACA GGC AGG GGT CCA-3', antisense: 5'-AAT ACT ATT TTC TGG TGG TTA GTT C-3'). Samples were heated to 94℃ for 3 min, 55℃ for 1 min, and 72℃ for 1 min and cycled 29 times through 94℃ for 30 sec, 55℃ for 1 min, and 72℃ for 1 min. The final incubation was at 72℃ for 7 min. The mixture was subjected to 2% agarose gel that for electrophoresis with the indicated markers and primers for the internal standard (GAPDH). Each sample was applied more than two lanes in the same gel. The agarose gel was stained with ethidium bromide and photographed with UV transillumination. The intensity of the bands was analyzed and quantified by computer-assisted densitometry using an NIH image. For the control, the different intensities of each band provided from the sample of C57BL/6J mice were analyzed, and the average intensity was calculated. Then, each control intensity was again compared with the average intensity to calculate the standard error. Under these conditions, each intensity of bonds for the sample obtained from CXBK mice was analyzed and compared with the average intensity of that from C57BL/6J mice. Finally, % of control was quantified as described in Chapter 2.

Assessment of antinociception

Antinociception was determined according to the method described in Chapter 2.

I.t. injection

I.t. administration was performed according to the method described previously [80] using a 25 μL Hamilton syringe with a 30 gauge needle. The injection volume was 4 μL for each mouse. Each solution was injected without injection cannulae.

Competitive displacement binding

For the membrane preparation, the spinal cords of mice were quickly removed 24 hr after repeated morphine (10 mg/kg, s.c.) injection and rapidly transferred to a tube filled with ice-cold buffer. The membrane homogenate was prepared as described previously [74]. Briefly, the dissected tissue was homogenized in ice-cold buffer containing 50 mM Tris-HCl (pH 7.4), 5 mM $MgCl_2$ and 1 mM ethylene glycol-bis (2-aminoethylether)-*N*,*N*,*N'*,*N'*-tetraacetic acid (EGTA). The homogenate was centrifuged at 1,000 x g for 10 min at 4 °C and the supernatant was ultracentrifuged at 48,000 x g for 20 min at 4 °C. The pellet was suspended in ice-cold assay buffer containing 50 mM HEPES (pH 7.4) and 2 mM $MgCl_2$ followed by centrifugation at 48,000 x g for 20 min at 4 °C. The resultant pellet was resuspended in ice-cold assay buffer and stored at -80 °C until used.

Binding affinities of morphine or fentanyl to MORs in the spinal cord of ICR mice were determined by competitive displacement binding with graded concentrations

(0.01-100 pM) of unlabeled morphine or fentanyl incubated with 1 nM [D-Ala^2,*N*-Me-Phe^4,Gly^5-ol]enkephalin (DAMGO) for 60 min at 25°C. Nonspecific binding was determined using 1 μM DAMGO. For all competitive binding assays, IC_{50} was determined from the displacement curves using a one-site model and nonlinear regression.

[^{35}S]GTPγS binding assay

[^{35}S]GTPγS binding assay was determined according to the method described in Chapter 2.

Statistical analysis

The data are presented as the mean ± S.E.M. The statistical significance of differences between the groups was assessed with Student's *t*-test or one-way ANOVA followed by Bonferroni/Dunnett test.

Results

Characterization of the antinociception induced by morphine or fentanyl

Morphine or fentanyl given s.c. produced antinociception, reaching maximal antinociceptive responses at 15 and 30 min, respectively, after the injection (data not shown). The antinociception induced by s.c. morphine (3 mg/kg) or fentanyl (30 μg/kg) was significantly attenuated by pretreatment with β-FNA (Fig. 1A). In contrast, NTI (selective δ-receptor antagonist) and nor-BNI (selective κ-receptor antagonist) had no effect on either morphine- or fentanyl-induced antinociception (Fig. 1A). The dose of NTI or nor-BNI used in the present study sufficiently antagonized antinociception produced by i.c.v.-administered DPDPE (selective δ-receptor agonist) or s.c.-administered U-50,488H (selective κ-receptor agonist), respectively (Fig. 1A). When opioid antagonists were administered at the doses used in the present study, these antagonists did not produce any changes in the basal tail-flick latency (data not shown).

The supraspinal antinociception induced by either i.c.v.-administered morphine or fentanyl was markedly suppressed by pretreatment with β-FNA (Fig. 1B). Furthermore, the i.t.-administered morphine- or i.t.-administered fentanyl-induced antinociception was significantly attenuated by β-FNA (Fig. 1C). Maximal antinociceptive effect of morphine or fentanyl was observed at 10-15 min or 5 min, respectively, following each injection (data not shown).

Comparison of ED_{50} values for antinociceptive effects induced by morphine or

fentanyl when given s.c., i.c.v. or i.t.

As shown in figure 2, s.c., i.c.v. or i.t. administration of either morphine or fentanyl produced significant antinociceptive effects in a dose-dependent manner. In the present study, I determined the ED_{50} values for s.c.-, i.c.v.- and i.t.-administered fentanyl- or morphine-induced antinociception (Table 1). In morphine-treated groups, the ED_{50} values for s.c., i.c.v. and i.t. administrations were 2.58 μmol/kg, 1.85 nmol/mouse and 0.13 nmol/mouse, respectively. In fentanyl-treated groups, the ED_{50} values for s.c., i.c.v. and i.t. administrations were 0.035 μmol/kg, 0.10 nmol/mouse and 0.11 nmol/mouse, respectively. The ED_{50} values for fentanyl-induced antinociceptive effects following s.c., i.c.v. and i.t. injections were shown in Table 1. The morphine (MRP)/fentanyl (FEN) ratio for s.c., i.c.v. or i.t. route was 73.7, 18.5 or 1.2, respectively.

Comparison of antinociceptive effects observed in CXBK and C57BL/6J mice at the supraspinal sites

The supraspinal antinociceptive effects of morphine (i.c.v.) or fentanyl (i.c.v.) in CXBK and their parental strain C57BL/6J mice were investigated using the tail-flick test (Fig. 3). In C57BL/6J mice, either morphine or fentanyl produced a dose-dependent antinociceptive effect. In contrast, CXBK mice significantly exhibited a weak antinociception induced by i.c.v. administration of both morphine and fentanyl as compared to that in C57BL/6J mice at the doses used in the present study. (**$p<0.01$ and ***$p<0.001$)

Binding affinity of morphine or fentanyl to spinal MORs in ICR mice

To evaluate the specific involvement of the opioid receptor types and MOR subtypes in antinociceptive properties of morphine and fentanyl, I determined the competitive displacement binding of [^{3}H]DAMGO with graded concentrations (0.01-100 pM) of unlabeled morphine or fentanyl. As shown in Fig. 4, [^{3}H]DAMGO binding to the membrane fraction obtained from the spinal cord of ICR mice was completely displaced by increasing concentrations of either morphine or fentanyl. The displacement curves for morphine or fentanyl was found to be nearly superimposed. The IC_{50} values for morphine and fentanyl were 2.02 and 2.47 nM, respectively. On the other hands, [^{3}H]DPDPE or [^{3}H]U69,593 binding to the membrane obtained from the mouse spinal cord or the cerebellum of guinea pig, respectively, was not affected by incubation with morphine or fentanyl (data not shown).

Reduction in the expression of MOR-1B mRNA in the spinal cord of CXBK mice as compared to that in their progenitor C57BL/6J mice

To investigate the expression of spliced variant-dependent MOR subtypes MOR-1, MOR-1B and overall MORs mRNAs in the spinal cord of CXBK mice, I carried out semi-quantitative analysis of each mRNA using RT-PCR assay. In the present study, CXBK mice display a significant reduction in the expression of either MOR or MOR-1B mRNA in the spinal cord as compared to that in their progenitor C57BL/6J mice (Fig. 5A and B). In the preliminary study, I confirmed that the expression of MOR-1B

mRNA was completely abolished in MOR gene knockout mice (unpublished observation). In contrast, there was no significant difference in MOR-1 production between the two strains (Fig. 5C).

Comparison of the spinal antinociceptive effect and G-protein activation induced by morphine or fentanyl between CXBK and C57BL/6J mice

I examined the spinal antinociceptive effects induced by morphine or fentanyl in CXBK mice (Fig. 6A and B). Either morphine (0.1-1.0 nmol/mouse) or fentanyl (0.17-3.0 nmol/mouse) when given i.t. induced a dose-dependent antinociceptive effect in C57BL/6J mice (ED_{50}: 0.27 or 0.41 nmol/mouse, respectively). In contrast, CXBK mice exhibited significantly a weak antinociception induced by i.t. administration of morphine or fentanyl as compared to that in C57BL/6J mice (ED_{50}: 3.31 or 5.04 nmol/mouse, respectively) (morphine: $F(1, 364)=17.84$, ***$p<0.001$, fentanyl: $F(1, 90)=120.20$, ***$p<0.001$). The dose-response line for antinociceptive effects of morphine or fentanyl in C57BL/6J mice was significantly shifted to right by 12.4- or 12.2-fold in CXBK mice, respectively. I next compared the activation of G-protein induced by morphine or fentanyl between CXBK and C57BL/6J mice (Fig. 6C and D). Either morphine or fentanyl (0.001-10 μM) produced a concentration-dependent increase in the binding of [^{35}S]GTPγS to spinal cord membranes obtained from C57BL/6J mice. In CXBK mice, the binding of [^{35}S]GTPγS stimulated by either morphine or fentanyl was significantly decreased compared to that in C57BL/6J mice. The EC_{50} values for morphine in CXBK and C57BL/6J mice were 77.45 and 5.55 μM,

respectively. On the contrary, the EC_{50} values for fentanyl in CXBK and C57BL/6J mice were 32.50 and 3.31 μM, respectively. The EC_{50} values for G-protein activation induced by either morphine or fentanyl in C57BL/6J mice were significantly enhanced by 13.9- or 9.8-fold in CXBK mice, respectively.

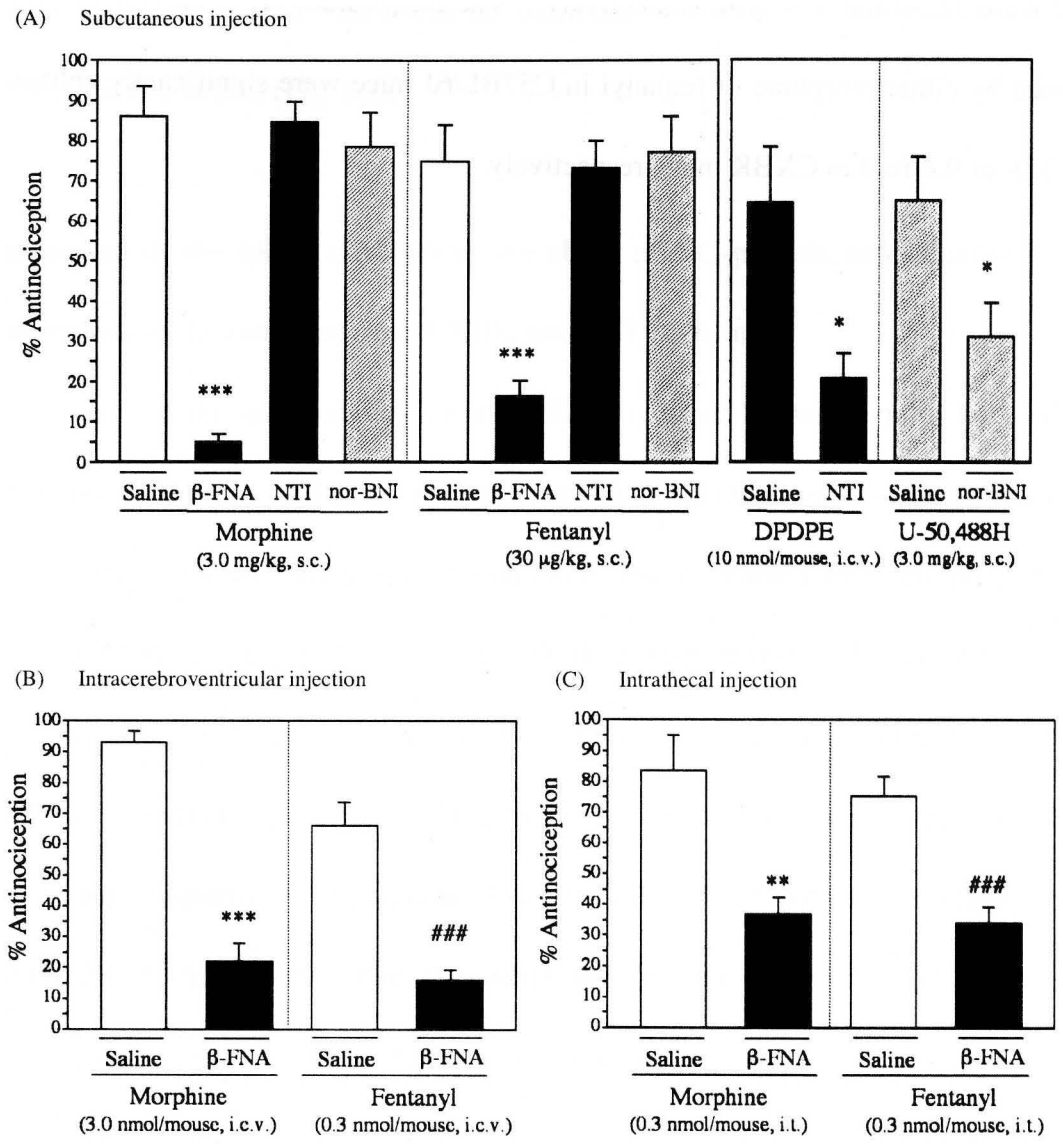

Fig. 1 (A) *Left panel:* Effects of β-FNA, NTI or nor-BNI on s.c. morphine (MRP)- or fentanyl (FEN)-induced antinociception in the mouse tail-flick test. *Right panel:* Effects of NTI or nor-BNI on i.c.v. [D-Pen^2, Pen^5]enkephalin (DPDPE)- or s.c. U-50,488H-induced antinociception in the tail-flick test. β-FNA (40 mg/kg), NTI (3 mg/kg) or nor-BNI (3 mg/kg) was administered s.c. 24 hr, 30 min or 4 hr before s.c. administration of agonists. *p< 0.05 and ***p< 0.001 vs. saline-pretreated groups. (B) Effects of β-FNA on i.c.v. MRP- or FEN-induced antinociception in the mouse tail-flick test. β-FNA (40 mg/kg) was administered s.c. 24 hr before s.c. administration of agonists. ***p< 0.001, ###p< 0.001 vs. respective agonist alone. (C) Effects of β-FNA on i.t. MRP- or FEN-induced antinociception in the mouse tail-flick test. β-FNA (40 mg/kg) was administered s.c. 24 h before s.c. administration of agonists. ***p< 0.01, ###p< 0.001 vs. respective agonist alone. Each bar represents the mean ± S.E.M. of 10-15 mice.

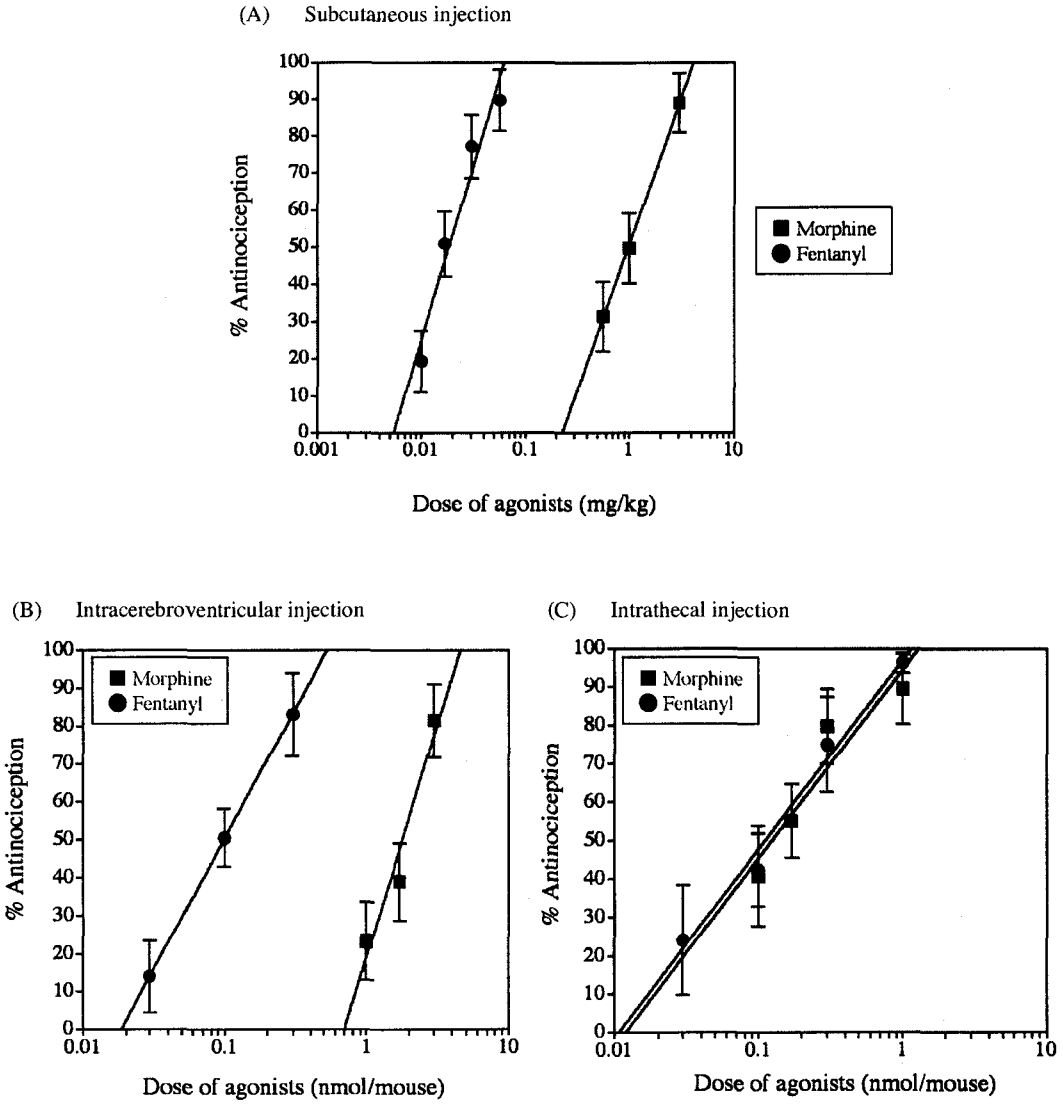

Fig. 2 The antinociceptive effect induced by s.c. (A), i.c.v. (B) and i.t. (C) injection of morphine or fentanyl in ICR mice. The mouse tail-flick assay was performed at 10 or 5 min after i.t. injection of morphine or fentanyl. Each point represents the mean ± S.E.M. of 12 mice for each group.

Table 1 Antinociceptive effects of fentanyl (FEN) and morphine (MRP)

ED_{50} values were determined by Litchfield-Wilcoxon analysis. To calculate ED_{50}, at least 3 drug doses were used and 8-15 mice were used for each dose. Values in parenthesis indicate the 95 % confidence range.

Injection site	ED_{50} values		MRP/FEN ratio
	Agonist		
	FEN	MRP	
s.c.	0.035 μmol/kg (0.025-0.049)	2.58 μmol/kg (1.37-4.85)	73.7
i.c.v.	0.10 nmol/mouse (0.04-0.23)	1.85 nmol/mouse (1.17-2.92)	18.5
i.t.	0.11 nmol/mouse (0.05-0.25)	0.13 nmol/mouse (0.06-0.28)	1.2

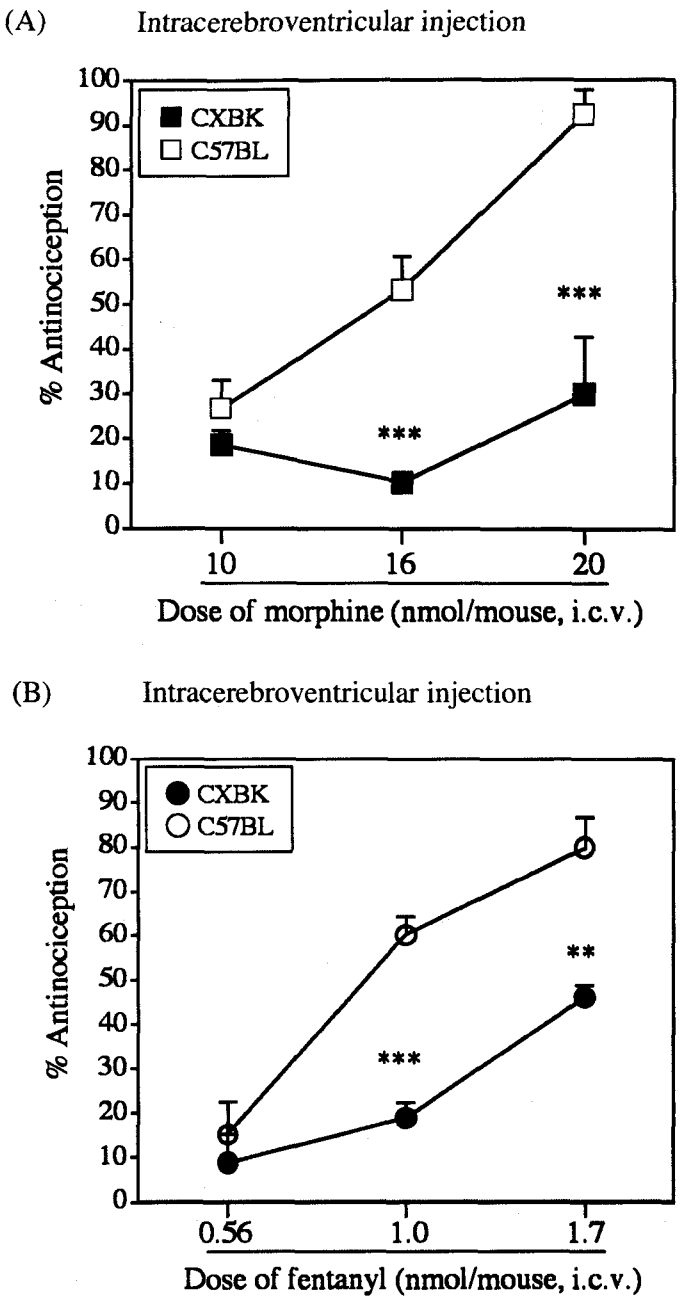

Fig. 3 The dose-response curve for antinociceptive effect induced by i.c.v. injection of morphine (A) or fentanyl (B) in CXBK and C57BL/6J (C57BL) mice. Antinociception was expressed as a percentage of maximum possible effect (% Antinociception). Each point represents the mean ± S.E.M. of 5-6 mice. ***p< 0.001, ##p< 0.01 and ###p< 0.001 vs. C57BL mice.

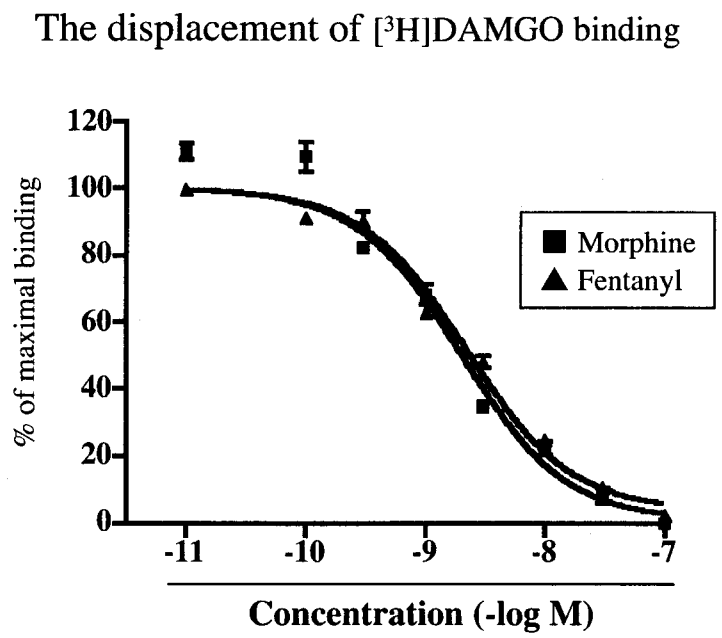

Fig. 4 Comparison of binding affinities of morphine and fentanyl determined from competitive displacement binding against [^{3}H]DAMGO in spinal membranes of ICR mice. Competitive displacement binding by morphine or fentanyl was performed incubating spinal membranes with 1 nM [^{3}H]DAMGO in the presence of graded concentrations (0.01-100 pM) of unlabeled morphine or fentanyl. Nonspecific binding was determined using 1 μM DAMGO. For all competitive binding assays, IC_{50} was determined from the displacement curves. Values in parenthesis indicate the 95 % confidence range.

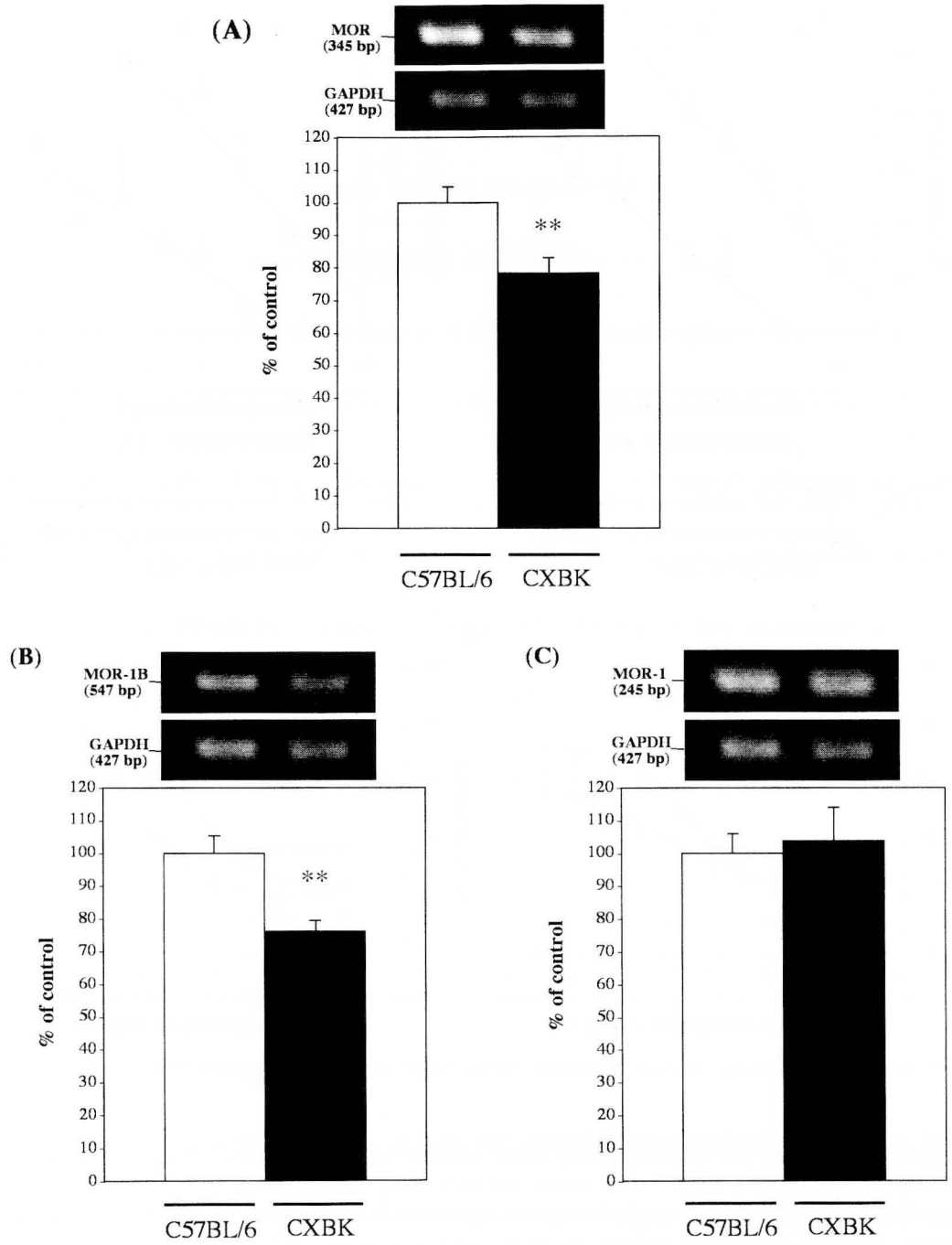

Fig. 5 Reduced expression of MOR-1B mRNA in the spinal cord of CXBK mice. *Upper*: Representative RT-PCR for overall MORs (A), MOR-1B (B) and MOR-1 (C) mRNAs in the spinal cord obtained from C57BL/6J and CXBK mice. *Lower*: Semi-quantitation of the intensity of the each band. The sample mixture was subjected to 2% agarose gel electrophoresis with the indicated markers and primers for the internal standard GAPDH. Six experiments using three independent samples were performed in this study. The value for CXBK mice is expressed as a percentage against C57BL/6J mice. Each column represents the mean ± S.E.M. of six experiments. **p<0.01 vs. C57BL/6J mice.

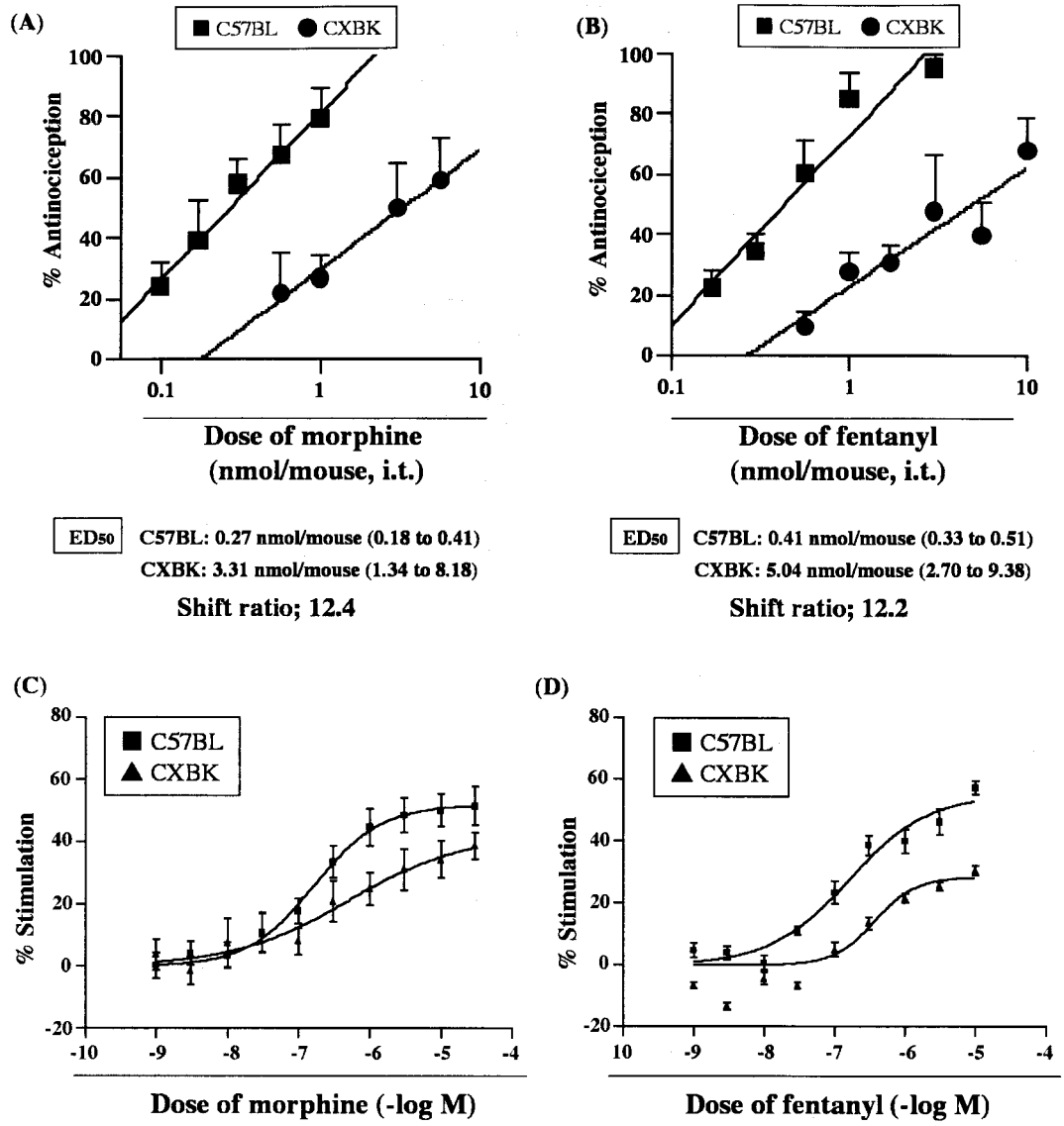

Fig. 6 (A) and (B) The antinociceptive effect induced by i.t. injection of morphine or fentanyl in CXBK and C57BL/6J mice. The mouse tail-flick assay was performed at 10 or 5 min after i.t. injection of morphine or fentanyl. Each point represents the mean with S.E.M. of 4-6 mice for each group. Values in parenthesis indicate the 95% confidence range. (C) and (D) Effect of morphine or fetanyl on the binding of [^{35}S]GTPγS to membranes of the spinal cord obtained from C57BL/6J and CXBK mice. Membranes were incubated with 50 pM [^{35}S]GTPγS and 30 μM GDP with or without different concentrations (0.1 nM-10 μM) of morphine or fentanyl. The data are expressed as a percentage of basal [^{35}S]GTPγS binding measured in the presence of GDP and absence of agonist. The data represent the mean ± SEM, at least, of three independent experiments. The F value of two-way ANOVA in morphine is F(1, 364)=17.84. ***p<0.001 vs. C57BL/6J mice. The F value of two-way ANOVA in fentanyl is F(1, 90)=120.20. ***p<0.001 vs. C57BL/6J mice.

Discussion

In the present study using the mouse tail-flick test, both morphine and fentanyl produced dose-dependent antinociceptive effects after s.c., i.c.v. or i.t. administration. These effects were significantly attenuated by pretreatment with the MOR antagonist β-FNA. The DOR antagonist NTI and KOR antagonist nor-BNI had no effects on antinociception induced by s.c. injection of morphine or fentanyl, whereas the dose of NTI or nor-BNI was sufficiently effective to inhibit the antinociceptive effect produced by DPDPE or U-50,488H. These findings indicate that either morphine or fentanyl induce antinociceptive effect via supraspinal and spinal MORs.

I determined the ED_{50} values for s.c., i.c.v. or i.t. injection of morphine- and fentanyl-induced antinociception in ddY mice. It is noteworthy that the MRP/FEN ratio for s.c. administration was much higher than that for i.t. and i.c.v. injections. These differences may result from their pharmacokinetic profiles. This notion can be supported by the finding that unlike morphine, fentanyl has a lipid-soluble profile and thus easily diffuses into the brain across the blood-brain barrier. This may be the major reason why s.c. injection of fentanyl can produce more potent antinociception than that of morphine. Furthermore, the present data provide further evidence for the usefulness of peripheral treatment with fentanyl as therapeutic strategies for the control of pain.

Next, I investigated the specific involvement of the opioid receptor types and MOR subtypes in analgesic properties of morphine and fentanyl. As mentioned in Chapter 2,

I demonstrated that CXBK strain can be classified as MOR-1B-knockdown mice, and that MOR-1B plays an important role in supraspinal antinociception of the endogenous MOR agonist endomorphin-1. In the present study, both morphine and fentanyl when given i.c.v. induced antinociception in outbred ddY mice and inbred C57BL/6J mice. Conversely, antinociceptive activity induced by i.c.v. administration of both morphine and fentanyl was much lower in CXBK mice, being in good agreement with the finding of endomorphin-1 in Chapter 2. These findings indicate that antinociceptive effects of i.c.v.-administered morphine and fentanyl are, at least in part, mediated through MOR-1B at the supraspinal site.

In order to further understand the roles of the opioid receptor types and MOR subtypes in the antinociceptive effects of morphine and fentanyl at spinal levels, I performed the competitive displacement binding study using [^{3}H]DAMGO. In the present study, no significant difference in the binding affinity to MORs in the mouse spinal cord was noted between morphine and fentanyl, pointing out the possibility that both morphine and fentanyl basically act on spinal MORs in the same manner. Next, I investigated the antinociceptive effects induced by i.t. administration of morphine or fentanyl in CXBK mice. In the present study, I demonstrated that CXBK mice display a significant reduction in the expression of MOR-1B mRNA in the spinal cord compared to that in their progenitor C57BL/6J mice. Furthermore, the expression of overall MOR mRNA is decreased in the spinal cord of CXBK mice. These findings are consistent with the previous report that the level of MOR mRNA in the brain of CXBK mice is reduced to approximately 60% of their progenitor mice [52]. In contrast,

the expression level of MOR-1 mRNA in the brain of CXBK mice was similar to that found in C57BL/6J mice. Thus, the present findings indicate a specific loss of MOR-1B mRNA expression in the spinal cord, as well as brain, of this strain. Under these conditions, it is of interest to note that either the spinal antinociceptive effect induced by morphine or fentanyl in C57BL/6J mice was significantly decreased in CXBK mice with the same degree. In addition, there was no significant difference between morphine and fentanyl on G-protein activation in MOR-1B knockdown CXBK mice. Taken together, the present findings suggest that MOR-1B may, at least in part, play a potential role in both morphine- and fentanyl-mediated spinal antinociception.

The large body of evidence suggests that the binding of structurally distinct ligands to GPCR including opioid receptors leads to the multiple changes of receptor conformation, which could trigger distinct signal pathway. [81-83] Considering these findings, although I could not provide evidence for the essential difference of mechanisms underlying spinal antinociceptive effects between morphine and fentanyl in the present study, there is a possibility that morphine and fentanyl shows the essential difference in the binding site of each agonist in MOR or agonist-MOR binding form, which could lead to the distinct change in MOR conformation and downstream signaling machinery. Alternatively, there is another possibility that morphine and fentanyl reveal the distinct reactivity to MOR subtypes excluding MOR-1B in the mouse spinal cord. To further understand the differences in molecular mechanisms underlying the antinociceptive effects between morphine and fentanyl, more experiments are needed to perform.

In conclusion, the present data provide the evidence that a lack of MOR-1B expression may, at least in part, contribute to the reduced sensitivity to morphine and fentanyl at either the supraspinal or spinal site of CXBK mice. Furthermore, MOR-1B may play a potential role in the MOR-mediated antinociception at both the supraspinal and spinal sites.

General conclusion

The above findings lead to the following conclusions:

In Chapter 1:

The anti-hyperalgesic effect induced by fentanyl in CFA-pretreated mice was rapidly disappeared during the consecutive administration of fentanyl, whereas morphine preserved its potency of anti-hyperalgesic effect. In addition, repeated treatment with fentanyl, but not morphine, resulted in the increase in levels of p-MOR associated with the enhanced inactivation of PP2A and the reduction in Rab4-dependent MOR resensitization. These findings point out the possibility that chronic treatment with fentanyl may cause the different modulation from chronic treatment with morphine on either the internalization or resensitization of MORs in the spinal cord under the pain-like state. The present data provide first evidence for the mechanism underlying the development of tolerance to fentanyl-induced anti-hyperalgesic effect under the chronic pain.

In Chapter 2:

Here I found for the first time that CXBK recombinant-inbred mice display a significant reduction in the expression of MOR-1B mRNA in the brain as compared to that in their progenitor C57BL/6J mice. Furthermore, relatively lower levels of MOR-1B-IR were detected in the PAG of CXBK mice than that observed in C57BL/6J mice.

Under these conditions, I found that the increased level of [^{35}S]GTPγS bindings to whole brain membranes induced by a selective MOR agonist endomorphin-1 was significantly decreased in CXBK mice, indicating that CXBK strain can be classified as MOR-1B-knockdown mice. In addition, the i.c.v. pretreatment with AS-ODN to exon 5 of MOR gene produced a significant reduction in the i.c.v.-administered endomorphin-1-induced antinociceptive effect, being in good agreement with the findings in CXBK mice. The present data provide the first evidence that a lack of MOR-1B expression may, at least in part, contribute to the reduced sensitivity to MOR agonists in CXBK mice, and that MOR-1B may play a critical role in the MOR-mediated supraspinal antinociception.

In Chapter 3:

In the present study using the mouse tail-flick test, the antinociceptive effects induced by s.c., i.c.v. or i.t. administration of either morphine or fentanyl were significantly attenuated by pretreatment with MOR antagonist β-FNA, confirming that either morphine or fentanyl induce antinociceptive effect via supraspinal and spinal MORs. Furthermore, CXBK mice exhibited a weak antinociception induced by i.c.v. administration of both morphine and fentanyl as compared to that in C57BL/6J mice at the doses used in the present study. In competitive displacement binding study using [^{3}H]DAMGO, no significant difference in the binding affinity to MORs in the mouse spinal cord was noted between morphine and fentanyl. Interestingly, RT-PCT assay showed that a specific loss of MOR-1B mRNA expression in the spinal cord of CXBK

mice. Under these conditions, it should be noted that either the spinal antinociceptive effect and G-protein activation induced by morphine or fentanyl in C57BL/6J mice were significantly decreased in CXBK mice with the same degree. Taken together, the present findings suggest that MOR-1B may, at least in part, play an important role in both morphine- and fentanyl-mediated supraspinal and spinal antinociception.

Working hypothesis

Based on the findings noted, I try to describe my hypothesis concerning the change in the spinal function following chronic morphine treatment (See Fig. A). Repeated treatment with fentanyl, but not morphine, resulted in the increase in levels of p-MOR associated with the enhanced inactivation of PP2A and the reduction in Rab4-dependent MOR resensitization. However, I could not detect the essential difference of mechanisms underlying spinal antinociceptive effects between morphine and fentanyl in the present study. It seems likely that these differences in tolerance to anti-hyperalgesic effects between chronic treatment with morphine and fentanyl under the pain-like state may result from the distinct reactivity between morphine and fentanyl to MOR subtypes excluding MOR-1B in the mouse spinal cord. Alternatively, the different pharmacological profile between morphine and fentanyl observed in the present study may reflect the essential difference of each MOR agonist in the the binding site of each agonist in MOR or agonist-MOR binding form, leading to the conformational changes in MOR at the spinal site. Although further experiments are needed to perform, the present findings provide the first evidence for the molecular

mechanism underlying the development of tolerance to fentanyl-induced anti-hyperalgesic effect under the chronic pain.

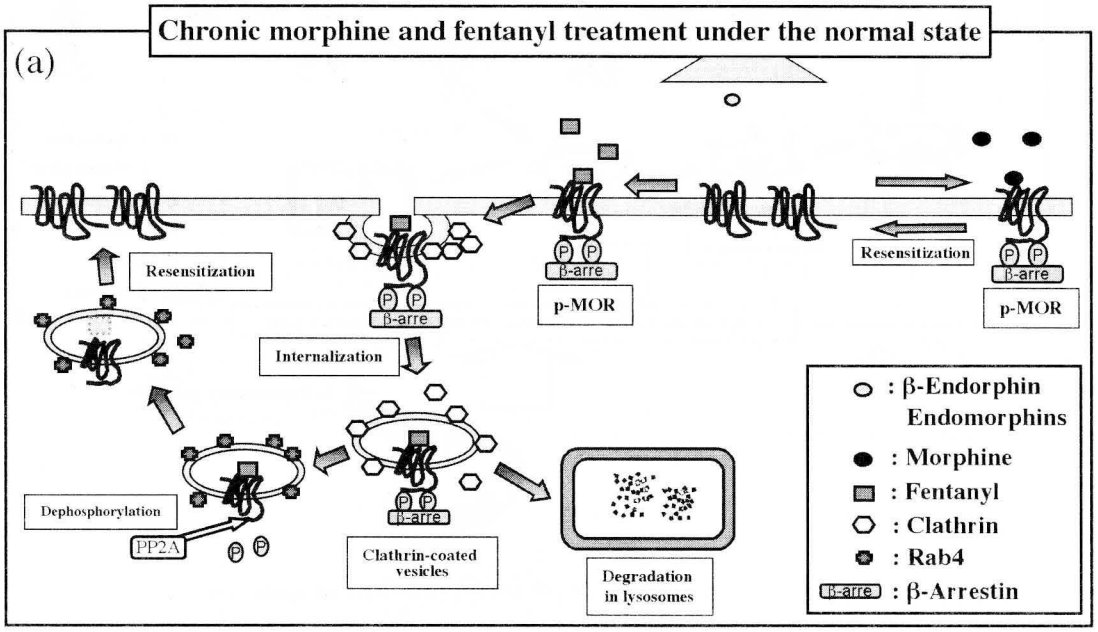
Chronic morphine and fentanyl treatment under the normal state
(a)
Resensitization
β-arre
p-MOR
Internalization
Dephosphorylation
PP2A
Clathrin-coated vesicles
Degradation in lysosomes
: β-Endorphin Endomorphins
: Morphine
: Fentanyl
: Clathrin
: Rab4
: β-Arrestin

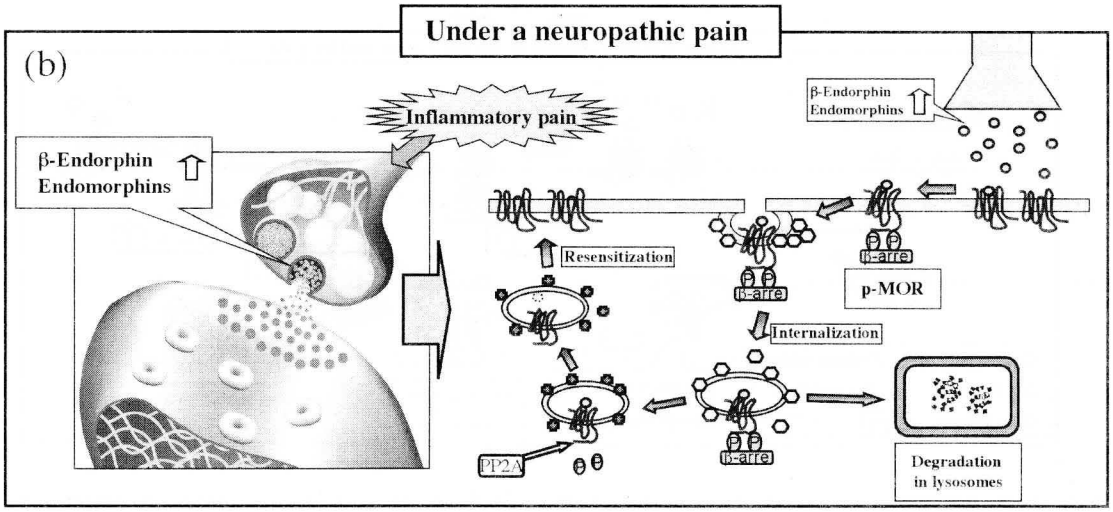
Under a neuropathic pain
(b)
Inflammatory pain
β-Endorphin Endomorphins
Resensitization
β-arre
p-MOR
Internalization
PP2A
Degradation in lysosomes

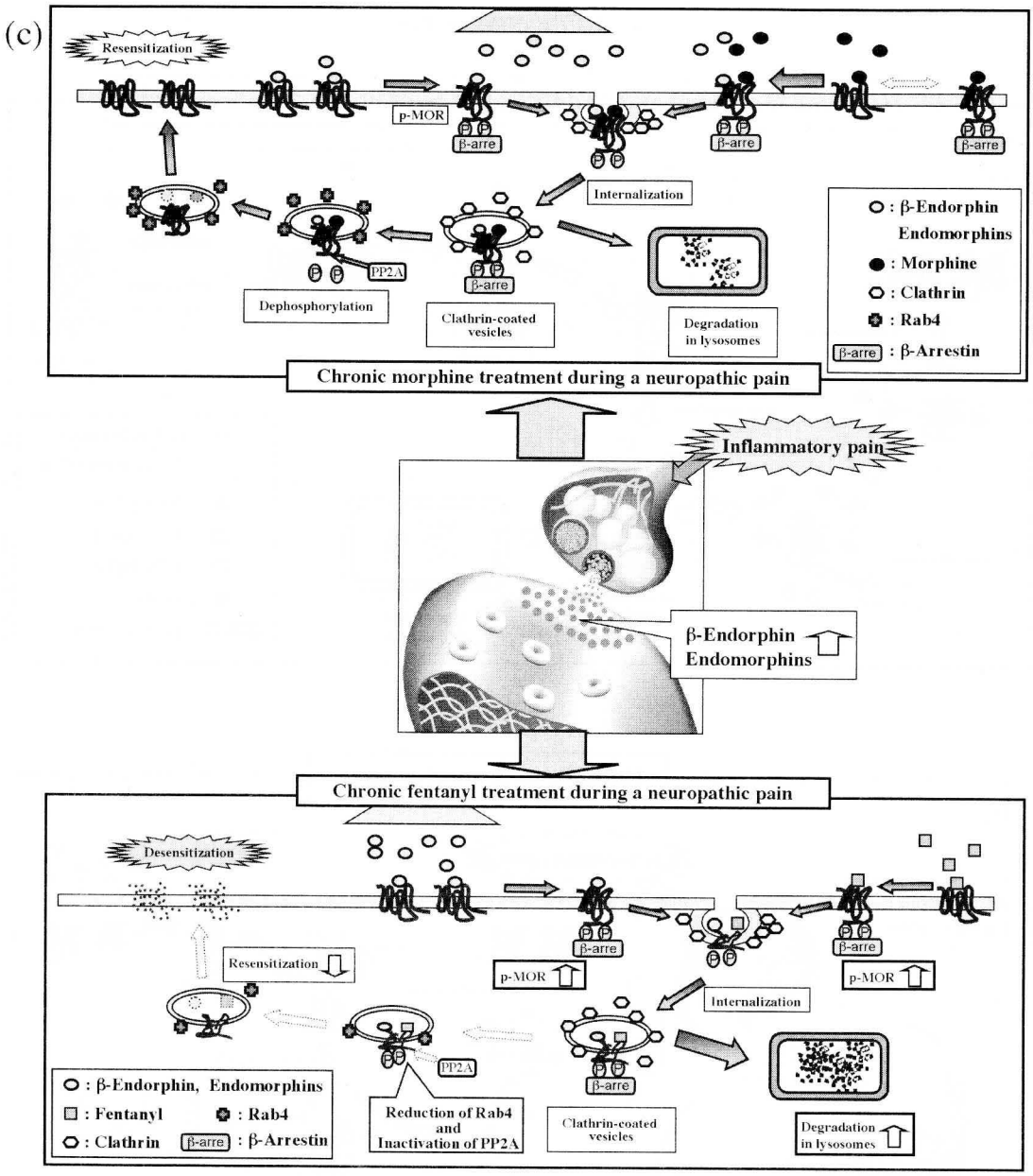

Fig. A (a) Schematic models of the μ-opioid receptor (MOR) turnover following chronic treatment with morphine or fentanyl. Fentanyl induces internalization of MORs. In contrast, morphine does not promote detectable internalization of MORs after repeated treatment, although it is well established that morphine induces the phosphorylation of MORs. (b) Schematic models of changes in the MOR turnover during a neuropathic pain. It has been considered that the release of endogenous MOR peptides such as β-endorphin and endomorphins is increased in the spinal cord during a neuropathic pain. It is reported that endogenous opioid peptides induce internalization of MORs (see in the reference 56). (c) Schematic models of the difference of mechanisms underlying tolerance to anti-hyperalgesic effects between chronic treatment with morphine and fentanyl under the pain-like state in the mouse spinal cord. See the detail in "Working hypothesis".

List of Publications

This dissertation is based on the following original publications:

1, Satoshi Imai, Minoru Narita, Seiko Hashimoto, Atsushi Nakamura, Kan Miyoshi, Hiroyuki Nozaki, Nana Hareyama, Tomoe Takagi, Masami Suzuki, Michiko Narita and Tsutomu Suzuki: Differences in tolerance to anti-hyperalgesic effects between chronic treatment with morphine and fentanyl under the pain-like state: Comparison between etorphine and morphine. Jpn J Neuropsychopharmacol (in press): Chapter 1 and 3

2, Minoru Narita, Satoshi Imai, Satoru Ozaki, Masami Suzuki, Michiko Narita and Tsutomu Suzuki: Reduced expression of a novel μ-opioid receptor (MOR) subtype MOR-1B in CXBK mice: implications of MOR-1B in the expression of MOR-mediated responses. Eur J Neurosci 18, 3193-3198 (2003): Chapter 2

3, Minoru Narita, Satoshi Imai, Yumiko Itou, Yoshinori Yajima and Tsutomu Suzuki: Possible involvement of μ_1-opioid receptors in the fentanyl- or morphine-induced antinociception at supraspinal and spinal sites. Life Sci 70, 2341-2354 (2002): Chapter 3

Acknowledgements

This research will never be materialized without the help of the following people and organization:

First, I would like to express my gratitude and appreciation to Professor Tsutomu Suzuki (Department of Toxicology, Hoshi University School of Pharmacy and Pharmaceutical Sciences) and Associate Professor Minoru Narita (Department of Toxicology, Hoshi University School of Pharmacy and Pharmaceutical Sciences) for their helpful guidance in my research work and preparing this dissertation, and for giving a chance of this research work.

I would like to thank Ms. Michiko Narita for her excellent technical assistance, helpful guidance and valuable advice in my research work.

I wish to thank Dr. Masami Suzuki for her helpful support and stimulating discussions in my research work. I would like to thank Mr. Kan Miyoshi, Ms. Seiko Hashimoto, Mr. Atsushi Nakamura for their helpful support in my research work. I wish to thank Dr. Yuya Ise, Dr. Hideaki Kato, Dr. Yoshinori Yajima, Dr. Takeshi Aoki, Dr. Mayumi Miyatake and Dr. Junaidi Khotib for their kindly guidance in my research work.

Also, I wish to thank all of graduate and undergraduate students of Department of Toxicology, Hoshi University School of Pharmacy and Pharmaceutical Sciences, especially Ms. Naoko Kuzumaki, Mr. Kazuya Miyagawa, Mr. Yasuyuki Nagumo, Mr. Keiichi Niikura, Mr. Keisuke Hashimoto, Ms. Kana Nanjo, Mr. Hiroyuki Nozaki, Ms. Nana Hareyama, Ms. Tomoe Takagi, Ms. Megumi Asato and Mr. Masahiro Shibasaki for their expert technical assistance and helpful support in my research work.

Furthermore, I would like to express my gratitude and appreciation to Professor Nobutaka Hattori (Department of Neurology, Juntendo University School of Medicine), Assistant professor Shinichiro Kubo (Department of Neurology, Juntendo University School of Medicine) and Mr. Taku Hatano (Department of Neurology, Juntendo University School of Medicine) for their kindly support.

Finally, I would like to express my gratitude to my parents, sister, wife Masumi and friends for their assistance in my life.

References

1) Lord J, Waterfield A, Hughes J and Kosterlitz H. Endogenous opioid peptides: Multiple agonists and receptors. *Nature* **267**, 495-499 (1977).

2) Chang K. and Cuatrescasas P. Multiple opiate receptors. Enkephalins and morphine binding to receptors of different specificity. *J Biol Chem* **254**, 2610-2618 (1979).

3) Paterson S, Robson L and Kosterlitz H. Classification of opioid receptors. *Br Med Bull* **39**, 31-36 (1983).

4) Evans CJ, Keith DEJr, Morrison H, Magendzo K and Edwards RH. Cloning of a delta opioid receptor by functional expression. *Science* **258**, 1952-1955 (1992).

5) Kieffer BL, Befort K, Gaveriaux-Ruff C and Hirth CG. The δ-opioid receptor: isolation of a cDNA by expression cloning and pharmacological characterization. *Proc Natl Acad Sci USA* **89**, 12048-12052 (1992).

6) Chen Y, Mestek A, Liu J, Hurley JA and Yu L. Molecular cloning and functional expression of a μ-opioid receptor from rat brain. *Mol Pharmacol* **44**, 8-12 (1993).

7) Wang JB, Imai Y, Eppler CM, Gregor P, Spivak CE and Uhl GR. μ Opiate receptor: cDNA cloning and expression. *Proc Natl Acad Sci USA* **90**, 10230-10234 (1993).

8) Meng F, Xie GX, Thompson RC, Mansour A, Goldstein A, Watson SJ and Akil H. Cloning and pharmacological characterization of a rat κ opioid receptor. *Proc Natl Acad Sci USA* **90**, 9954-9958 (1993).

9) Li S, Zhu J, Chen C, Chen YW, Deriel JK, Ashby B and Liu-Chen LY. Molecular cloning and expression of a rat κ opioid receptor. *Biochem J* **295**, 629-633 (1993).

10) Bunzow JR, Saez C, Mortrud M, Bouvier C, Williams JT, Low M and Grandy DK. Molecular cloning and tissue distribution of a putative member of the rat opioid receptor gene family that is not a μ, δ or κ opioid receptor type. *FEBS Lett* **347**, 284-288 (1994).

11) Chen Y, Fan Y, Liu J, Mestek A, Tian M, Kozak CA and Yu L. Molecular cloning, tissue distribution and chromosomal localization of a novel member of the opioid receptor gene family. *FEBS Lett* **347**, 279-283 (1994).

12) Xie YF, Wang J, Huo FQ, Jia H and Tang JS. μ but not δ and κ opioid receptor involvement in ventrolateral orbital cortex opioid-evoked antinociception in formalin test rats. *Neuroscience* **126**, 717-726 (2004).

13) Mao J, Price DD, Zhu J, Lu J and Mayer DJ. The inhibition of nitric oxide-activated poly(ADP-ribose) synthetase attenuates transsynaptic alteration of spinal cord dorsal horn neurons and neuropathic pain in the rat. *Pain* **72**, 355-366 (1997).

14) Nichols ML, Bian D, Ossipov MH, Lai J and Porreca. Regulation of morphine antiallodynic efficacy by cholecystokinin in a model of neuropathic pain in rats. *J Pharmacol Exp Ther* **275**, 1339-1345 (1995).

15) Murthy K and Makhlouf G. Opioid μ, δ, and κ receptor-induced activation of phospholipase C-β3 and inhibition of adenylyl cyclase is mediated by G_{i2} and G_o in smooth muscle. *Mol Pharmacol* **50**, 870-877 (1996).

16) Kramer HK and Simon EJ. Role of protein kinase C (PKC) in agonist-induced μ-opioid receptor down-regulation: I. PKC translocation to the membrane of SH-SY5Y neuroblastoma cells is induced by μ-opioid agonist. *J Neurochem* **72**, 585-593 (1999).

17) Fukuda K, Kato S, Morikawa H, Shoda T and Mori K. Functional coupling of the δ-, μ- and κ-opioid receptors to mitogen-activated protein kinase and arachidonate release in Chinese hamster ovary cells. *J Neurochem* **67**,1309-1316 (1996).

18) Goodman RR and Pasternak GW. Visualization of μ_1 opiate receptors in rat brain by using a computerized autoradiographic subtraction technique. *Proc Natl Acad Sci USA* **82**, 6667-6671 (1985).

19) Pasternak GW. Insights into mu opioid pharmacology: The role of μ opioid receptor subtypes. *Life Sci* **68**, 2213-2219 (2001).

20) Pan Y-X, Xu J, Mahurter L, Bolan E, Xu M and Pasternak GW. (2001) Generation of the μ opioid receptor (MOR-1) protein by three new splice variants of the *Oprm* gene. *Proc Natl Acad Sci USA* **98**, 14084-14089 (2001).

21) Zimprich A, Simon T and Hollt V. Cloning and expression of and isoform of the rat μ opioid receptor (rMOR1B) which differs in agonist induced desensitization from rMOR1. *FEBS Lett* **359**, 142-146 (1995).

22) Koch T, Schulz S, Schroder H Wolf R, Raulf E and Hollt V. Carboxyl-terminal splicing of the rat μ opioid receptor modulates agonist-mediated internalizaiton and receptor resensitization. *J Biol Chem* **273**, 13652-13657 (1998).

23) Wolf R, Koch T, Schulz S, Klutzny M, Schroder H, Raulf E, Buhling F and Hollt V. Replacement of threonine 394 by alanine facilitates internalization and resensitization of the rat μ opioid receptor. *Mol Pharmacol* **55**, 263-268 (1999).

24) Pan Y-X, Xu J, Bolan E, Abbadie C, Chang, A, Zuckerman A, Rossi G and Pasternak GW. Identification and characterization of three new alternatively spliced

μ-opioid receptor isoforms. *Mol Pharmacol* **56**, 396-403 (1999).

25) Abbadie C, Pan Y-X, Drake CT and Pasternak GW. Comparative immunohistochemical distributions of carboxy terminus epitopes from the μ-opioid receptor splice variants MOR-1D, MOR-1 and MOR-1C in the mouse and rat CNS. *Neuroscience* **100**, 141-153 (2000).

26) Abbadie C and Pasternak GW. Differential in vivo internalization of MOR-1 and MOR-1C by morphine. *Neuroreport* **12**, 3069-3072 (2001).

27) Craig AD. An ascending general homeostatic afferent pathway originating in lamina I. *Prog Brain Res* **107**, 225-242 (1996).

28) Han ZS, Zhang ET and Craig AD. Nociceptive and thermoreceptive lamina I neurons are anatomically distinct. *Nat Neurosci* **1**, 218-225 (1998).

29) Siddall PJ and Cousins MJ. Neuroral Blockade in Clinical Anesthesia and Management of Pain, **3rd edition**, Philadelphia, Lippinocott-Raven, 675-699 (1998).

30) Yen CT, Fu TC and Chen RC. Distribution of thalamic nociceptive neurons activated from the tail of the rat. *Brain Res* **498**, 118-122 (1989).

31) Casey KL, Minoshima S, Berger KL, Koeppe RA, Morrow TJ and Frey KA. Positron emission tomographic analysis of cerebral structures activated specifically by repetitive noxious heat stimuli. *J Neurophysiol* **71**, 802-807 (1994).

32) Beitel RE and Dubner R. Response of unmyelinated (C) polymodal nociceptors to thermal stimuli applied to monkey's face. *J Neurophysiol* **39**, 1160-1175 (1976).

33) Bessou P and Perl ER. Response of cutaneous sensory units with unmyelinated fibers to noxious stimuli. *J Neurophysiol* **32**, 1025-1043 (1969).

34) Woolf CJ. Evidence for a central component of post-injury pain hypersensitivity. *Nature* **308**, 686-688 (1983).

35) Seltzer Z, Dubner R and Shir Y. A novel behavioral model of neuropathic pain disorders produced in rats by partial sciatic nerve injury. *Pain* **43**, 205-218 (1990).

36) Kim SH and Chung JM. An experimental model for peripheral neuropathy produced by segmental spinal nerve ligation in the rat. *Pain* **50**, 355-363 (1992).

37) Wolfe GI and Trivedi JR. Painful peripheral neuropathy and its nonsurgical treatment. *Muscle Nerve* **30**, 3-19 (2004).

38) Ossipov MH, Lopez Y, Nichols ML, Bian D and Porreca F. The loss of antinociceptive efficacy of spinal morphine in rats with nerve ligation injury is prevented by reducing spinal afferent drive. *Neurosci Lett* **199**, 87-90 (1995).

39) Narita M, Kuzumaki N, Suzuki M, Narita M, Oe K, Yamazaki M, Yajima Y and Suzuki T. Increased phosphorylated-μ-opioid receptor immunoreactivity in the mouse spinal cord following sciatic nerve ligation. *Neurosci Lett* **354**, 148-152 (2004).

40) Ling GS, MacLeod JM, Lee S, Lockhart SH and Pasternak GW. Separation of morphine analgesia from physical dependence. *Science* **226**, 462-464 (1984).

41) Freye E and Latasch L. Development of opioid tolerance -- molecular mechanisms and clinical consequences. *Anasthesiol Intensivmed Notfallmed Schmerzther* **38**, 14-26 (2003).

42) Mather LE. Clinical pharmacokinetics of fentanyl and its newer derivatives. *Clin Pharmacokinet* **8**, 422-446 (1983).

43) Sittl R, Nuijten M and Poulsen Nautrup B. Patterns of dosage changes with

transdermal buprenorphine and transdermal fentanyl for the treatment of noncancer and cancer pain: A retrospective data analysis in Germany. *Clin Ther* **28**, 1144-1154 (2006).

44) Lefkowitz RJ. G protein-coupled receptors. III. New roles for receptor kinases and beta-arrestins in receptor signaling and desensitization. *J Biol Chem* **273**, 18677-18680 (1998).

45) Claing A, Laporte SA, Caron MG and Lefkowitz RJ. Endocytosis of G protein-coupled receptors: roles of G protein-coupled receptor kinases and beta-arrestin proteins. *Prog Neurobiol* **66**, 61-79 (2002).

46) Bohm SK, Grady EF and Bunnet NW. Regulatory mechanisms that modulate signaling by G-protein-coupled receptors. *Biochem J* **322**, 1-18 (1997).

47) Wang JM, Ali H, Richardson R, Snyderman R and Oppenheim JJ. Opiates transdeactivate chemokine receptors: δ and μ opiate receptor-mediated heterologous desensitization. *J Exp Med* **188**, 317-325 (1998).

48) Schulz S, Mayer D, Pfeiffer M, Stumm R, Koch T and Hollt V. Morphine induces terminal μ-opioid receptor desensitization by sustained phosphorylation of serine-375. *EMBO J* **23**, 3282-3289 (2004).

49) Haeseler G, Foadi N, Ahrens J, Dengler R, Hecker H and Leuwer M. Tramadol, fentanyl and sufentanil but not morphine block voltage-operated sodium channels. *Pain* **In press** (2006).

50) Moskowitz AS and Goodman RR. Autoradiograpic distribution of μ_1 and μ_2 opioid binding in the mouse central nervous system. *Brain Res* **360**, 117-129 (1985).

51) Roy B, Cheng RSS, Phelan J and Pomeranz B. Pain threshold and brain endorphin levels in geneticallu obese (ob/ob) and opiate receptor deficient (CXBK) mice. In: Way EL, editor. *Endogeneous and Exogeneous Opiate Agonists and Antagonists.* New York: Pergamon., 297-300 (1979).

52) Ikeda K, Ichikawa T, Kobayashi T, Kumanishi T, Oike S and Yano R. Unique behavioural phenotypes of recombinant-inbred CXBK mice: partial deficiency of sensitivity to μ- and κ-agonists. *Neurosci Res* **34**, 149-155 (1999).

53) Ikeda K, Kobayashi T, Ichikawa T, Kumanishi T, Niki H and Yano R. The untranslated region of μ-opioid receptor mRNA contributes to reduced opioid sensitivity in CXBK mice. *J Neurosci* **15**, 1334-1339 (2001).

54) Belke-Louis GF, Wehmeyer A and Schulz R. μ-opioid receptor expression in high five insect cells is regulated by 5' untranslated region (5'UTR). *Life Sci* **64**, 913-921 (1999).

55) Mizoguchi H, Narita M, Wu H, Narita M, Suzuki T, Nagase H and Tseng LF. Differential involvement of μ_1-opioid receptors in endomorphin- and β-endorphin-induced G-protein activation in the mouse pons/medulla. *Neuroscience* **100**, 835-839 (2000).

56) Minnis JG, Patierno S, Kohlmeier SE, Brecha NC, Tonini M and Sternini C. Ligand-induced μ opioid receptor endocytosis and recycling in enteric neurons. *Neuroscience* **119**, 33-42 (2003).

57) Narita M, Mizoguchi H, Narita M, Nagase H, Suzuki T and Tseng LF. Involvement of spinal protein kinase Cγ in the attenuation of opioid μ-receptor-mediated G-protein

activation after chronic intrathecal administration of [D-Ala^2, N-MePhe^4, Gly-Ol^5]enkephalin. *J Neurosci* **21**, 3715-3720 (2001).

58) Ammon-Treiber S and Hollt V. Morphine-induced changes of gene expression in the brain. *Addict Biol* **10**, 81-89 (2005).

59) Chakrabarti S, Regec A and Gintzler AR. Chronic morphine acts via a protein kinase Cγ-Gβ-adenylyl cyclase complex to augment phosphorylation of Gβ and Gβγ stimulatory adenylyl cyclase signaling. *Brain Res Mol Brain Res* **138**, 94-103 (2005).

60) Yoshikawa M, Nakayama H, Ueno S, Hirano M, Hatanaka H and Furuya H. Chronic fentanyl treatments induce the up-regulation of μ opioid receptor mRNA in rat pheochromocytoma cells. *Brain Res* **859**, 217-223 (2000).

61) Runnegar M, Wei X, Berndt N and Hamm-Alvarez SF. Transferrin receptor recycling in rat hepatocytes is regulated by protein phosphatase 2A, possibly through effects on microtubule-dependent transport. *Hepatology* **26**, 176-185 (1997).

62) Ward ES, Martinez C, Vaccaro C, Zhou J, Tang Q and Ober RJ. From sorting endosomes to exocytosis: association of Rab4 and Rab11 GTPases with the Fc receptor, FcRn, during recycling. *Mol Biol Cell* **16**, 2028-2038 (2005).

63) Standifer KM and Pasternak GW. G proteins and opioid receptor-mediated signalling. *Cell Signal* **9**, 237-248 (1997).

64) Wolozin BL and Pasternak GW. A classification of multiple morphine and enkephalin binding sites in the central nervous system. *Proc Natl Acad Sci USA* **78**, 6181-6185 (1981).

65) Ling GSF, Spiegel K, Lockhart SH and Pasternak GW. Naloxonazine actions in

vivo. *Eur J Pharmcol* **129**, 33-38 (1986).

66) Stefano GB, Goumon Y, Casares F, Cadet P, Fricchione GL, Rialas C, Peter D, Sonetti D, Guarna M, Welters ID and Bianchi E. Endogenous morphine. *Trends Neurosci* **23**, 436-442 (2000).

67) Pasternak GW. Incomplete cross tolerance and multiple μ opioid peptide receptors. *Trends Pharmacol Sci* **22**, 67-70 (2001).

68) Matthes HWD, Maldonado R, Simonin F, Valverde O, Slowe S, Kitchen I, Befort K, Dierich A, Menr ML, Dolle P, Tzavara E, Hanoune J, Roques BP and Kiffer BL. Loss of morphine-induced analgesia, reward effect and withdrawal symptoms in mice lacking the μ-opioid receptor gene. *Nature* **383**, 819-823 (1996)

69) Sora I, Takahashi N, Funada M, Ujike H, Revay RS, Donovan DM, Miner LL and Uhl GR. Opiate receptor knockout mice define μ receptor roles in endogenous nociceptive responses and morphine-induced analgesia. *Proc Natl Acad Sci USA* **94**, 1544-1549 (1997).

70) Narita M, Mizoguchi H, Narita M, Sora I, Uhl GR and Tseng LF. Absence of G-protein activation by μ-opioid receptor agonists in the spinal cord of μ-opioid receptor knockout mice. *Br J Pharmacol* **126**, 451-456 (1999).

71) Chen H-C, Seybold VS and Loh HH. An autoradiographic study in μ-opioid receptor knockout mice. *Mol Brain Res* **76**, 170-172 (2000).

72) Moskowitz AS and Goodman RR. Autoradiographic analysis of mu1, mu2 and delta opioid binding in the central nervous system of C57BL/6BY and CXBK (opioid receptor-deficient) mice. *Brain Res* **360**, 108-116 (1985).

73) Narita M, Imai S, Itou Y, Yajima Y and Suzuki T. Possible involvement of μ1-opioid receptors in the fentanyl- or morphine-induced antinociception at supraspinal and spinal sites. *Life Sci* **70**, 2341-2354 (2002).

74) Narita M, Mizoguchi H, Suzuki T, Narita M, Dun NJ, Imai S, Yajima Y, Nagase H, Suzuki T and Tseng LF. Enhanced μ-opioid responses in the spinal cord of mice lacking protein kinase Cγ isoform. *J Biol Chem* **18**, 15409-15414 (2001)

75) Brown HE, Garcia MM and Harlan RE. A two focal plane method for digital quantification of nuclear immunoreactivity in large brain areas using NIH-image software. *Brain Res Protoc* **2**, 264-272 (1998).

76) Narita M, Mizoguchi H, Narita M, Nagase H, Suzuki T and Tseng LF. Involvement of spinal protein kinase Cγ in the attenuation of opioid μ-receptor-mediated G-protein activation after chronic intrathecal administration of [D-Ala^2, N-MePhe^4, Gly-Ol^5]enkephalin. *J Neurosci* **21**, 3715-3720 (2001).

77) Haley MJ and McCormick WG. Pharmacological effects produced by intracerebral injections of drugs in the conscious mouse. *Br J Pharmacol* **12**, 12-5 (1957).

78) Zimprich A, Simon T and Hollt V. Transfected rat μ opioid receptors (rMOR1 and rMOR1B) stimulate phospholipase C and Ca^{2+} mobilization. *Neuroreport* **7**, 54-56 (1995).

79) Goldberg IE, Rossi GC, Letchworth SR, Mathis JP, Ryan-Moro,J., Leventhal L, Su W, Emmel D, Bolan EA and Pasternak GW. Pharmacological characterization of endomorphin-1 and endomorphin-2 in mouse brain. *J Pharmacol Exp Ther* **286**, 1007-1013 (1998).

80) Hylden JL and Wilcox GL. Intrathecal morphine in mice: a new technique. Eur J Pharmacol **67**, 313-316 (1980).

81) Brys R, Josson K, Castelli MP, Jurzak M, Lijnen P,Gommeren W and Leysen JE. Econstitution of the human 5-HT_{1D} receptor-G-protein coupling: evidence for constitutive activity and multiple receptor conformations. *Mol Pharmacol* **57**, 1132-1141 (2000).

82) Robb S, Cheek TR, Hannan FL, Hall LM, Midgley JM and Evans PD. Agonist-specific coupling of a cloned Drosophila octopamine/tyramine receptor to multiple second messenger systems. *EMBO J* **15**, 1325-1330 (1994).

83) Wreggett KA and Wells JW. Cooperativity manifest in the binding properties of purified cardiac muscarinic receptors. *J Biol Chem* **270**, 22488-22499 (1995).